



Multiobjective energy efficient street lighting framework: A data analysis approach

Pragna Labani Sikdar¹ · Samarjit Kar² · Parag Kumar Guha Thakurta¹

Accepted: 15 February 2022 / Published online: 1 April 2022

© The Author(s), under exclusive licence to Springer Science+Business Media, LLC, part of Springer Nature 2022

Abstract

A data analysis approach for designing an energy efficient street lighting framework is proposed to maximize both energy efficiency and uniformity of the system. A multiobjective optimization problem on obtaining energy efficiency is formulated in a comprehensive manner. Three multiobjective evolutionary optimization algorithms such as nondominated sorting genetic algorithm II, strength Pareto evolutionary algorithm 2 and multiobjective differential evolutionary algorithm are used to analyse the approximated Pareto solutions of our proposed model. The performance of considered algorithms are presented and compared with regard to different metrics. The results from the best algorithm, in terms of convergence and diversity, among the algorithms are then validated using DIALux to ensure the recommendation for the standardization in different aspects. The proposed work contributes a comprehensive data analysis on genetic algorithm solutions towards obtaining a multiobjective energy efficient street lighting which is beyond the scope of the existing works. The results obtained by the proposed method are also compared with existing DIALux results. The improvement of energy efficiency obtained by the proposed methodology over existing works is shown in terms of various aspects.

Keywords Street lighting · Energy efficiency · Multiobjective optimization · Evolutionary algorithms · DIALux

1 Introduction

Street lighting is considered an important component of total illumination used across the world. It has been increasing globally at a rate of 3–6% per year [1]. This lighting system provides safety for passersby and vehicles at night as well as plays a major role in reducing crime [2]. However, as per the technical report in [3], the street lighting system is also responsible for consuming a huge amount of electrical energy. It consumes almost 40% of the total electricity required for a city. Every year, about 114 TeraWatt Hour (TWh) is consumed by the street lighting system [4]. It is observed that the reduction in electricity consumption

for lighting can result into a major reduction of the entire electricity consumption from 19% to 11% [5]. For these concerns, it has become necessary to preserve electrical energy to install the street lights in an energy efficient manner without violating the safety of the users.

In general, the street lights are positioned on the road depending on the design parameters related to the installation of the lighting system [6]. However, this methodology does not facilitate an energy efficient system, where the designer needs to focus on the least energy usage with sufficient illumination. Furthermore, the installation of street lighting should follow the recommendation of the International Commission on Illumination (CIE) and the European Committee for Standardization [7, 8]. In this context, the designers use DIALux [9], an open source software program used for lighting installation, to follow these recommendations. Nowadays, advanced methodologies have been adopted to install the lighting system for fulfilling the efficiency requirement [10]. Fortunately, there is a growing interest for many researchers to apply several optimization algorithms for the development of the street lighting system. However, it is unfaithful to design an energy efficient street lighting system in a single objective manner as it is usually

✉ Pragna Labani Sikdar
ps.18cs1107@phd.nitdgp.ac.in

¹ Department of Computer Science & Engineering, NIT Durgapur, Durgapur, West Bengal, 713209, India

² Department of Mathematics, NIT Durgapur, Durgapur, West Bengal, 713209, India

involved with multiple issues related to the street condition. Even, in some cases, these become contradictory objectives corresponding to each other.

Several multiobjective evolutionary algorithms (MOEAs) are used to develop an energy efficient lighting system. For example, the energy efficiency of the street lights is maximized by applying differential evolutionary algorithm (DEA) [6]. In this article [6], they have focused only on a single objective, which is not sufficient for the design of a street lighting system. Hence, nondominated sorting genetic algorithm II (NSGAI) is applied in [11] to maximize the efficiency of the system by considering multiple objectives. However, finding the best algorithm among all possible MOEAs is beyond scope until and unless the performance metrics are determined. In some scenarios, the convergence or diversity is considered as performance metrics, while both can be used for measuring performance of the system under other circumstances [12]. Therefore, it is unwell to set only one or two metrics to determine its superiority among the existing algorithms as it can specify only a single qualification while neglecting the other in different aspects [13]. Furthermore, as per our best knowledge, till now MOEA based work is limited to the performance evaluation of a specific algorithm for its own in the design of street lighting system. Therefore, to make fair comparisons among different MOEAs in the street lighting system, a data analysis [13] framework is motivated to present here, so that it can provide suitable information to the designers for installing the street lights according to the requirement based on the street conditions and so on.

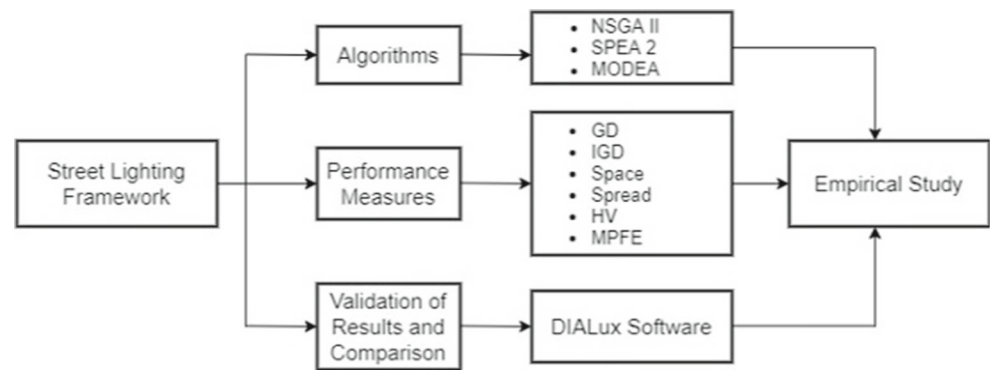
In this paper, a data analysis approach for designing an energy efficient street lighting framework is proposed to maximize both the efficiency and uniformity of the system using the parameters recommended by the CIE. Here, the efficiency is determined in terms of energy i.e., sufficient illumination must be preserved with less energy usage. Another aspect is regarding uniformity which refers to the consistency of the illumination level emitted from a light source i.e., there should not be a large difference in the values of minimum and average illumination of a light source on a specific location of the street. Here, both objectives are contradictory since improving one objective will degrade the performance of another. Hence, different MOEAs such as NSGAI, strength Pareto evolutionary algorithm 2 (SPEA2) and multiobjective DEA (MODEA) are used to develop the framework of energy efficient street lighting. These algorithms are used for various combination of the lighting classes and subclasses recommended by the CIE. Also, these lighting classes are considered for various installation design, such as one-sided and two-sided configuration. The performance of these MOEAs is determined by the convergence and diversity of the algorithmic solutions. Since, there is no true Pareto front

available for street lighting in the literature, hence an approximate front is generated that is close to the Pareto front. Then, the algorithms that are more converged to this approximate front is considered as most energy efficient, while the algorithms with more diversity provide more choices of solutions to install the lighting system. In this work, the value of six performance metrics such as Generational Distance (GD), Inverted Generational Distance (IGD), space, spread, Hypervolume (HV) and Maximum Pareto Front Error (MPFE) are evaluated for three proposed MOEAs to obtain a statistical analysis on convergence and diversity. Here, GD and MPFE determine the convergence and the rest of the metrics are used for diversity measurements. Significant comparative results with respect to these performance metrics are shown to highlight the convergence and diversity of the MOEAs which in turn emphasize energy efficiency in the street lighting framework. The energy efficient solutions obtained by the proposed framework is validated using DIALux. Furthermore, these solutions obtained by the proposed work are compared with DIALux results. The improvement of energy efficiency obtained by the proposed work over other existing approaches [6, 14–16] is shown in terms of various aspects. The evaluation of the proposed framework shown in Fig. 1 is highlighted for better understanding at a glance. The major contributions of the proposed work are summarized as follows:

- A street lighting framework is proposed to maximize energy efficiency and uniformity of the system.
- A multiobjective optimization (MOO) problem on obtaining energy efficient street lighting system is formulated in a comprehensive manner.
- Three MOEAs such as NSGAI, SPEA2 and MODEA are discussed towards obtaining the Pareto optimal solution for the problem addressed here.
- A data analysis approach related to performance metrics such as GD, IGD, space, spread, HV and MPFE is used for performance comparison among three MOEAs in terms of convergence and diversity.
- In terms of convergence and diversity, the outcomes from the best algorithm among the MOEAs are then validated using DIALux to ensure the recommendation for the standardization in different aspects. Furthermore, these results obtained from the proposed work are compared with existing DIALux results.
- An improved energy efficiency obtained by the proposed work over other existing approaches are shown.

The remaining of this paper is organized as: a literature survey in connection to the proposed work is discussed in Section 2. Preliminaries related to street lighting are discussed in Section 3 for ease of further discussions. Section 4 presents the formulation of the proposed work in this paper. The solution methodology for the proposed

Fig. 1 Evaluation framework [13] of the proposed energy efficient street lighting



model is described in Section 5. Performance measures of MOEAs are discussed in Section 6. Section 7 shows various simulation results followed by a conclusion in Section 8.

2 Literature survey

Nowadays, obtaining efficient energy in street lighting from various aspects is desirable in current research. Installation of public street lighting should be efficient in terms of energy as well as it should maintain comfort and safety to the users [4]. Hence, many researchers have contributed their work in designing an energy efficient lighting system by applying several techniques, which includes sensor based as well as different machine learning techniques. In one of our early works [17], a minimum threshold of the power requirement is obtained based on some infrastructural parameters for installing the streetlights. An adaptive lighting system is proposed in [18] that dynamically adjusts the brightness of the luminaries by detecting the presence of vehicles or pedestrians and therefore, a streetlight utility model is presented accordingly. The energy consumption of the streetlights presented in [18] is reduced in [19] by varying the inter-distance between two luminaries, which changes the time period of the lights to be lit. A detail analysis of different lighting schemes in connection to energy efficiency are presented in [14]. Another work on street lighting is discussed in [20] to obtain efficient energy in accordance with several infrastructural parameters like height of the pole, distance between two consecutive poles, width of the road etc. Measurement of lighting levels and associated parameters by an intelligent method is implemented in [16]. Again, the authors in [21] have studied the impact of energy consumption and subsequent effect in the atmosphere by replacing traditional ones with Light Emitting Diode (LED) based lights as it consumes less energy. It saves up to 90% of the electricity, maintaining the same comfort level. Street lighting with LED technology is redesigned by DIALux in [22] to provide better illumination. In other works [15, 23], the energy efficiency of the streetlights is determined

with respect to several street conditions. An efficient energy for the deployment of streetlights is approached with the help of a performance indicator [24]. In the context of the street lighting, an Artificial Neural Network (ANN) model is discussed in [25] where a training procedure is performed manually by setting the number of neurons on hidden layers. However, the energy reduction is beyond the scope of their work. Another ANN model is discussed in [4] to predict the energy consumption of the streetlights for different traffic volumes. In [26], a neural network model is used on a data set to provide an industrial management system. The work in [27] is focused on street light monitoring systems to reduce energy consumption along with less maintenance costs. An intelligent approach is presented in [28] to use gentle information. Another intelligent multiobjective algorithm in [29] is proposed in order to optimize the energy performance of the system.

Several MOEAs are used for the design of the street lighting framework. For example, GA is adopted in [30] to allocate the street lights in spite of the faulty scenarios in lighting. In another article [11], the concept of NSGAII is used for the maximization of several parameters of the lighting system related to the installation. Similarly, NSGAII is applied to maximize similar objectives in [31] based on the relationship between street lighting parameters as per CIE. In [32], a finding on the suitable solution related to street lighting installation among a large set of different configurations is discussed by MOEA. Another MOEA is presented in [33] in terms of genetic operators and dominance method. A MOO problem is addressed in [34] to combine the cost parameters under consideration of a useful factor. An application of MOO in this regard is discussed in [35]. In order to minimize energy consumption in street lighting using minimal infrastructure, another method is presented in [36] with an assurance of the quality. DEA is used in [6] to maximize the energy efficiency of the street lighting system by ignoring other related parameters. Thus, the work in [6] leads to a gap in completeness on an aspect of optimization. Again, SPEA2 is applied in [37] to predict energy performance in a system. However,

from our knowledge best, SPEA2 is not explored till now for the development of street lighting system. Furthermore, these existing works do not use the evolutionary techniques including GA as a data analysis tool [38].

In short, several procedures to obtain an energy efficient street lighting system are discussed in various aspects. However, regarding the question of optimization, it is unfair to indicate the solutions unless and until the suitable performance metrics are determined. It needs to be complete by approaching the suitability of those performance metrics as per user requirements or even depending on street conditions. As per our best knowledge, no prior work based on the utilization of data analysis is there for designing a street lighting framework. Therefore, the aim of the proposed work is to bring off a comparative study on the major performance metrics by data analysis on GA solutions. Subsequently, it can highlight their effectiveness to discover information for suggestive decision-making capability related to the deployment of energy efficient street lighting. Hence, a data analysis approach is proposed in this paper, where the performance of the model is evaluated with respect to a complete set of metrics for a possible combination of various parameters related to different lighting classes. For strengthening the data analysis, an ANOVA [39] test is carried out for the set of metrics addressed in this work. This would be transparent from successive discussions.

3 Street lighting preliminaries

In order to develop the street lighting system, it is essential to consider the relationship among various parameters associated with the lighting system according to the recommendation of the CIE. Some important terminologies, installation configuration and lighting classes are described here.

3.1 Terminologies used

- **Luminous flux** : It is a measurement of the brightness emitted from the light source. The unit of luminous flux is *lumens (lm)*.
- **Luminous intensity** : It is defined as the amount of luminous flux per unit solid angle in specific direction. It is measured in *candela (cd)*, i.e., *lumens/steradian*.
- **Luminance (L)** : It is defined as emitted luminous flux for a given angle which is calculated by candela per square meter (cd/m^2).
- **Illuminance (E)** : It is defined as the received luminous flux per unit surface and is measured in *lux (lx)* which is equivalent to *lumen/m²*.

- **Average illuminance or luminance (E_{av} or L_{av})** : The average value of E or L is required to be the minimum values of both throughout the lifetime of the respective light, which is denoted by E_{av} or L_{av} respectively.
- **Uniformity (U_0)** : Uniformity refers to the consistency of the value of E_{av} or L_{av} on the area to be lit. It is denoted by U_0 and the value of minimum illuminance or luminance of a luminari on unit surface of area should be close to the value of E_{av} or L_{av} respectively for maintaining a better uniformity.
- **Energy efficiency (ϵ)** : Energy efficiency refers to the minimization of energy consumption of the light source while the performance is not compromised. The energy efficiency (ϵ) of the street lighting system is measured in terms of power density indicator (D_p), where D_p is the inverse of ϵ i.e., $\epsilon = 1/D_p$. According to the European committee for standardization 2015 (CEN EN 13201: 2015) [8], D_p can be expressed in terms of E_{av} with respect to different sub-areas (i) by the following:

$$D_p = \frac{P}{\sum_{i=1}^n E_{av_i} \times A_i} \quad (1)$$

Here, 'P' is the maximum power of the luminaries, 'n' represents the total number of sub-areas (i) and 'A' denotes the area of the illuminated surface. It is known that if the light source is not a point source, then the large source can be assumed as the summation of many point sources. Very often, the illuminated surface is not perpendicular to the direction of light. In such a scenario, according to the laws of illumination [40], the illuminated area (A) is increased by a factor of the angle towards the direction of a light source and hence the illumination (E_{av}) is also decreased. Thus the value of D_p in (1) is estimated using E_{av_i} and A_i for different sub-areas (i) of an illuminated surface A . According to [8], the value of D_p determines the energy class of the corresponding installation, as shown in Table 1.

3.2 Installation configuration

The installation of the lighting system is dependent on the street width (ω) and the luminary height (H). Based on different values of ω and H , the design of a lighting system is classified into three major types such as *one-sided*, *two-sided staggered* and *two-sided coupled*. These are shown in Fig. 2, where, 'A' denotes the area covered by the emitted light source and the value of A is determined as follows:

$$A = \frac{\omega \times S}{k} \quad (2)$$

Table 1 Energy classes with corresponding values of D_p

Energy class	D_p [W/(lx.m ²)]
A	0.000-0.014
B	0.015-0.024
C	0.025-0.034
D	0.035-0.044
E	0.045-0.054
F	0.055-0.064
G	0.065-0.074

Where, ‘S’ represents the inter-distance between two luminaries and ‘k’ is the installation design factor. Here the value of $k = 1$ and $k = 2$ denote *one-sided* and *two-sided* installation respectively.

From the law of illumination [40], it can be stated that illumination on the road surface is decreased with increasing height of the light source. Hence, to avoid loss in luminous intensity, street lights are installed on both side of the road, where ω is greater than height (H) of the luminaries.

3.3 Lighting classes

According to the recommendation of CIE, there can be three different lighting classes based on the traffic volumes, road users, number of cross-sections in the road etc. These lighting classes are further divided into different subclasses, as shown in Table 2. These are briefly discussed next.

- *P (Pedestrian and low speed areas) lighting class:* It is installed in considerably low traffic and pedestrian areas and its performance is based on E_{av} . According to CIE, the minimum value of U_0 for this lighting class is 0.20.
- *C (Conflict areas) lighting class:* It is installed in conflict areas with heavy traffic volumes and its performance of C class is based on E_{av} . The minimum value of U_0 for this lighting class is 0.40.
- *M (Motorized areas) lighting class:* M class is generally installed in preferably less conflict areas where low speed motor vehicles pass in a moderate amount. Here,

the performance is based on L_{av} and the minimum value of U_0 is different for various subclasses.

4 Problem formulation

It is already discussed that the objective of the proposed work is to maximize the energy efficiency (ϵ) and uniformity (U_0) of the lighting system. Based on these objectives, the proposed work is formulated as discussed next.

It is known that, the installation of street lights falls into different energy classes based on the values of D_p as shown in Table 1. Here, it is observed that the class “A” is the most efficient while the energy class “G” is the least as the least value of D_p denotes the most efficient lighting system. In other words, it can be stated that, the maximization of ϵ can be achieved by minimizing the value of D_p .

The proposed work considers direct illumination from the street lights while neglecting the other sources of reflected indirect illumination. Moreover, the system considers *two-sided* installation configuration for those streets where value of ω becomes greater than value of H . Hence, the decrease of illuminance due to the law of illumination is neglected in the proposed work and value of E_{av} is assumed to be consistent for different sub-areas(i) of the total illuminated surface (A) for a single luminari. Thus, the value of D_p for the entire area is revised in (3) by considering (1) and (2) as follows:

$$D_p = \frac{P \times k}{E_{av} \times \omega \times S} \tag{3}$$

The uniformity (U_0) of the lighting system refers to the consistency of the illuminance level that affects the overall quality of the lighting. This U_0 can be quantified in terms of different lighting parameters of the system as:

$$U_0 = -\beta_0 - \beta_1 \times S + \beta_2 \times H - \beta_3 \times \omega + \beta_4 \times E_{av} \tag{4}$$

In (4), β_i s are the lighting parameters provided by the manufacturers and H refers the height of the luminaries that is dependent on both ω and k . It is to be noted here that the designers must follow the recommendation to maintain the quality of the lighting system. For example, it is essential for

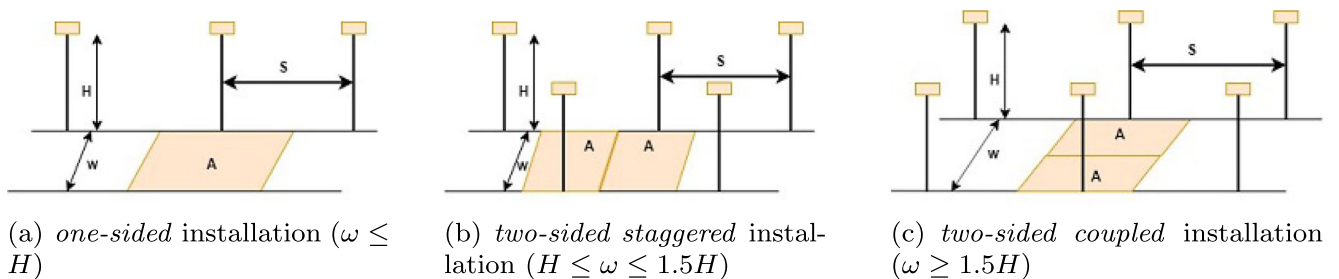


Fig. 2 Types of installation configuration (a) *one-sided*, (b) *two-sided staggered* and (c) *two-sided coupled*

Table 2 CIE recommended values of E_{av} and U_0 for the lighting classes

P Class			C Class			M Class		
Class	E_{av} (lx)	U_0	Class	E_{av} (lx)	U_0	Class	L_{av} (cd/m ²)	U_0
–	–	–	C0	50	0.40	–	–	–
P1	15	0.20	C1	30	0.40	M1	2.0	0.40
P2	10	0.20	C2	20	0.40	M2	1.5	0.40
P3	7.5	0.20	C3	15	0.40	M3	1.0	0.40
P4	5.0	0.20	C4	10	0.40	M4	0.75	0.40
P5	3.0	0.20	C5	7.5	0.40	M5	0.50	0.35
P6	2.0	0.20	–	–	–	M6	0.30	0.35

U_0 to have a minimum value 0.40 to install a lighting class C1 as shown in Table 2.

Under such scenarios, for the proposed work, the parameters of the lighting installation are considered as $X = \{x_1, x_2, x_3, x_4, x_5\}$ where, ‘ X ’ denotes a set of parameters. Here, x_1, x_2, x_3, x_4 and x_5 denote the values of inter-distance (S), luminari height (H), road width (ω), average illuminance (E_{av}) and maximum power of the luminari (P) respectively. Hence, the proposed work is formulated by the following:

$$\text{Objectives} \begin{cases} \text{Minimize } f_1(x) = \frac{x_5 \times k}{x_4 \times x_3 \times x_1} & (5) \\ \text{Maximize } f_2(x) = \sum_{i=0}^4 (-1)^i \beta_i x_i & (6) \end{cases}$$

subject to:

$$\bullet \quad x_3 \leq x_2, \forall k = 1 \quad (7)$$

$$\bullet \quad x_3 \leq x_2 \leq 1.5x_3, \forall k = 2 \quad (8)$$

$$\bullet \quad k \in \{1, 2\}, x_i \in X \forall i \in \{1, \dots, 5\}, x_0 = -1 \quad (9)$$

Here, the objective functions in (5) and (6) represent the minimization of D_p and the maximization of U_0 respectively. Here $x_0 = -1$ is considered for the sake of simplicity. Constraints given in (7) and (8) refer to the *one-sided* installation for $k = 1$ and the *two-sided* installation configuration for $k = 2$ respectively. The domain of other variables are defined in constraint (9).

5 Proposed methodology

In the proposed street lighting framework, it is unfaithful to design the system in a single objective manner as it is involved with several interrelated parameters related to the street lighting. Here, our objective functions are minimization of D_p and maximization of U_0 , as shown in (5) and (6). From (3) and (4), it is observed that increasing values of

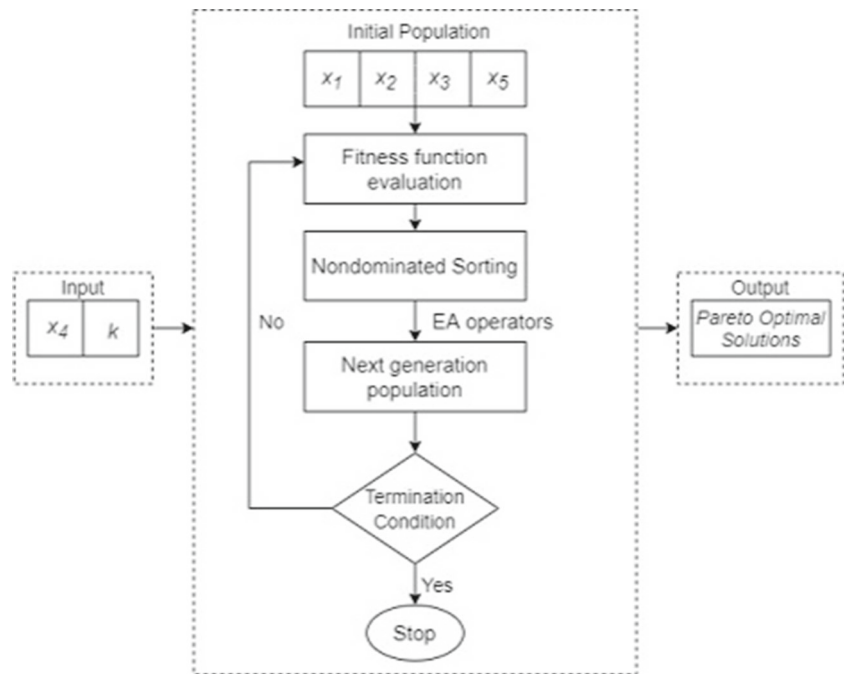
the parameters ω and S leads to the improvement of the objective function (5) while worsening the performance of objective function (6). Under this scenario, the use of several MOEA techniques can determine a set of nondominated Pareto optimal solutions which are beneficial in design of the street lighting framework according to different requirements. In the proposed model, the system takes the value of average illumination (E_{av}) and the installation design factor (k) as a set of input parameters $\{x_4, k\}$. Initially, the MOEA algorithms generate a set of random population where, each individual of the population consists of a set of combination of the lighting parameters $\{x_1, x_2, x_3, x_5\}$ as addressed earlier. After that, it evaluates the fitness function of each individual. Here, in the proposed methodology, the fitness values of the individuals are determined by D_p and U_0 , as shown in (3) and (4). This fitness evaluation is essential for the processing of next generation population. The populations with lesser values of D_p and higher values of U_0 are selected for the next generation by nondominated sorting process. This sorting process sorts the population according to the fitness values of the individual population. In next step, the evolutionary algorithm (EA) operators such as selection, crossover and mutation operations are applied to generate the child population i.e., the next generation population. This process continues until the termination condition is satisfied and the final population becomes the Pareto optimal solutions. This entire procedure of the proposed methodology is shown by a flowchart in Fig. 3.

The mechanism of the EA operators applied in the proposed work as shown in Fig. 3 are discussed next.

– Crossover

The crossover operation can explore the search space. Here, two individuals are selected randomly from initial population as parents and changes some of the genes to generate a new population known as child. In the proposed methodology, the crossover operation is performed based on a random matrix (α) as the size of

Fig. 3 Flowchart of the proposed methodology



the parent chromosome, as shown in Fig. 4a. Here, two parent population are shown as P1 and P2 and the child chromosome C1 and C2 are generated as follows:

$$\text{Child} \begin{cases} C1 = \alpha \cdot *P1 + (1 - \alpha) \cdot *P2 & (10) \\ C2 = \alpha \cdot *P2 + (1 - \alpha) \cdot *P1 & (11) \end{cases}$$

– Mutation

Mutation is another process of searching for new solutions in the search space. Unlike crossover, mutation operation alters only one gene of the parent population to search for a new solution in a local space. The mechanism of the mutation operation in the proposed methodology is shown in Fig. 4b. Here, σ is a parameter derived by the mutation rate of the MOEAs used in the proposed methodology and $j = 2$ is the position of the gene that is being altered to generate the child solution. The child solution is generated as follows:

$$C(j) = P(j) + \sigma \cdot *randn(\text{size}(j)) \quad (10)$$

5.1 MOEAs used

In the proposed work, three MOEAs such as NSGAI, SPEA2 and MODEA are used to solve the problem addressed earlier. All of these three MOEAs are applied to obtain a set of Pareto optimal solutions by following the working procedure as discussed in Fig. 3. However, the mechanism of the EA operators discussed earlier is different for MODEA than NSGAI and SPEA2 used here. So, a brief discussion

on NSGAI, SPEA2 and MODEA are discussed next for completeness of the work.

5.1.1 NSGAI

NSGAI is a nondominated sorting based MOEA that sorts the solutions, including the parents as well as the child population, at every iteration and finds the best solution among them. Thus, it preserves the elitism of the solutions [41]. Again, NSGAI preserves diversity by maintaining the crowding distance of the solutions at every iteration.

Initially, a random population is created by a set of solution and this population is known as parent population (P_t). Then the EA operators are used to generate the child population (Q_t). After that, combining P_t and Q_t , a frontification process determines a new population that becomes eligible for the next generation parent population (P_{t+1}). Here, such frontification process provides the solutions in different fronts by nondominated sorting. The first front ($F1$) denotes nondominated solutions over others. It dominates the solutions of the second front ($F2$) and so on. In the next step, the crowding distance of the solutions is calculated to maintain the diversity and the solutions with higher crowding distance are eligible for becoming as next generation parent population. These steps are continued until the termination condition, as per requirement, is reached and the corresponding $F1$ is considered as the Pareto optimal solutions. This entire procedure of the NSGAI approach is described by a pseudocode shown in Table 3.

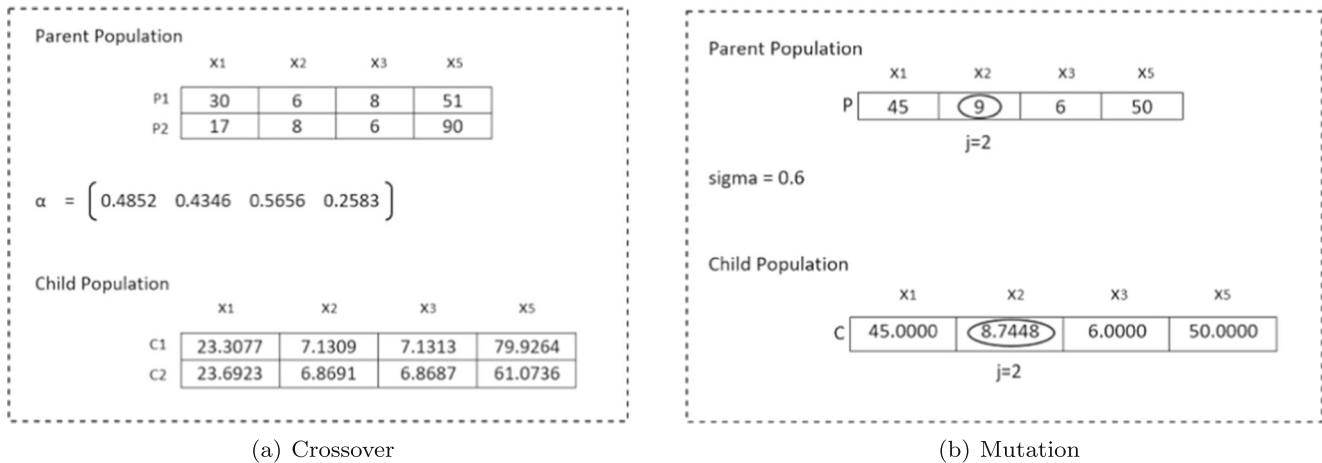


Fig. 4 Mechanism of the EA operators (a) Crossover and (b) Mutation

5.1.2 SPEA 2

SPEA2 is another well known MOEA technique which is involved in finding strength Pareto and fitness value for every individual of the solutions [42]. Unlike NSGA II, the focus on SPEA 2 is only on convergence, and diversity is not preserved here [43]. The algorithm is used for identifying a set of nondominated solutions and store it into an external set known as an archive and update it at every iteration.

Initially, it creates a random population (P_t) of size N and simultaneously, the archive (\bar{P}_t) is set to null at iteration $t = 0$. In the next step, a fitness value (F) is assigned to every

individual for both P_t and \bar{P}_t . After that, all nondominated solutions from both P_t and \bar{P}_t are copied to \bar{P}_{t+1} . Here, a condition is checked for the size of \bar{P}_{t+1} is greater or less than the archive size (\bar{N}). If the size of \bar{P}_{t+1} is greater than \bar{N} , then a truncation operation [44] is performed to reduce the size of \bar{P}_{t+1} , otherwise, \bar{P}_{t+1} is filled with dominated solution from P_t and \bar{P}_t . After that, the EA operators are applied to the individuals of \bar{P}_{t+1} to create the next generation population P_{t+1} . At the point of satisfying termination condition, the solutions of the archive set \bar{P}_t is considered as the Pareto optimal set. This process of the SPEA2 approach is described by a pseudocode shown in Table 4.

Table 3 NSGAI pseudocode

NSGAI(P)
<p>Begin NSGAI</p> <p>Input : Population (P_t) of size N at generation $t = 0$.</p> <p>Output : First nondominated front (F_1).</p> <p>Apply selection, crossover and mutation to generate child population Q_t for $t = 0$.</p> <p>while $t \leq$ maximum generation</p> <p style="padding-left: 20px;">$R_t = P_t \cup Q_t$</p> <p style="padding-left: 20px;">Calculate fitness value for every individual of R_t.</p> <p style="padding-left: 20px;">Apply nondominated sorting to generate nondominated fronts F_i for $i = 1, 2, \dots, n$.</p> <p style="padding-left: 20px;">while size of $(P_{t+1} \cup F_i) \leq N$</p> <p style="padding-left: 40px;">$P_{t+1} = P_{t+1} \cup F_i$</p> <p style="padding-left: 40px;">$i = i + 1$</p> <p style="padding-left: 20px;">end while</p> <p style="padding-left: 20px;">Calculate crowding distance of F_i.</p> <p style="padding-left: 20px;">$x \leftarrow$ size of P_{t+1}</p> <p style="padding-left: 20px;">$P_{t+1} = P_{t+1} \cup F_i[1 : (N - x)]$</p> <p style="padding-left: 20px;">Perform selection, crossover and mutation on P_{t+1} to generate Q_{t+1}.</p> <p style="padding-left: 20px;">end while</p> <p>End NSGAI</p>

Table 4 SPEA2 pseudocode

SPEA2(P)
<p>Begin SPEA2</p> <p>Input : A random population (P_t) of size N.</p> <p>Output : \bar{P}_t.</p> <p>Initialize : An archive set $\bar{P}_t = \Phi$ of size \bar{N} at generation $t = 0$.</p> <p>while $t \leq$ maximum generation</p> <p style="padding-left: 20px;">Calculate fitness value for every individual of P_t and \bar{P}_t.</p> <p style="padding-left: 20px;">Apply nondominated sorting on P_t and \bar{P}_t.</p> <p style="padding-left: 20px;">Copy all nondominated solutions from P_t and \bar{P}_t to \bar{P}_{t+1}.</p> <p style="padding-left: 20px;">if (size of \bar{P}_{t+1}) $\leq \bar{N}$</p> <p style="padding-left: 40px;">Copy dominated solutions from P_t and \bar{P}_t until \bar{P}_{t+1} is full.</p> <p style="padding-left: 20px;">else</p> <p style="padding-left: 40px;">Apply truncation operation to remove elements from \bar{P}_{t+1}.</p> <p style="padding-left: 20px;">end if</p> <p style="padding-left: 20px;">Perform selection, crossover and mutation on P_t to generate P_{t+1}.</p> <p>end while</p> <p>End SPEA2</p>

5.1.3 MODEA

This MOEA is involved with the generation of mutant vector and trial vector for mutation and crossover operations respectively [6]. Multiobjective Differential Evolutionary (MODE) is a variant of DEA which maintains convergence and diversity by nondominated sorting and crowding distance calculation [45]. However, repetitive nondominated sorting at every iteration may reduce the size of the population. To overcome this issue, trigonometric mutation operation is enhanced in MODEA [46].

Initially, a random set of population, also known as target vector (X), is generated with population size N_p . Then, the fitness value is calculated for every target vector X_i for $i = 1 \dots N_p$. After that, a nondominated sorting is performed and the resulting solution is passed to the DE operators. In the next step, trigonometric mutation operation is applied to obtain the mutant vector (V_i) according to each target vector X_i . After the mutation operation, a trial vector (Y_i) is generated for each individual X_i . The value of Y_i is same as V_i whenever a randomly generated number in the range of $[0,1]$ is less than or equal to a predefined crossover rate (CR), otherwise Y_i gets the value of X_i . In the next step, the crossover operation is performed based on the value of X_i , V_i and Y_i and the trial vector is updated accordingly. Now, the best solution between the trial vector and the target vector is selected as the next generation population. This process continues until the termination condition is satisfied and the final target vector X_i becomes the solution of the algorithm. This entire procedure of the MODEA approach is described by a pseudocode shown in Table 5.

5.2 Algorithm of the proposed methodology

In order to obtain an energy efficient street lighting, the proposed methodology considers three MOEAs for obtaining the Pareto optimal solutions of the objective functions as discussed earlier. Here, an approximate Pareto front (PF_{approx}) is generated, to determine the effectiveness of the performance of these MOEAs, which is close to the true Pareto front. To generate the PFapprox, the solutions of the first fronts ($F1$) obtained from NSGAI, SPEA2 and MODEA are combined which is treated as the initial population (P). Then, a crossover and mutation operation are performed on these solutions to generate the child population (C). In the next step, nondominated sorting and crowding distance assignment are performed on R , which is generated by combining the population P and C . This process continues until the termination condition is reached. Henceforth, a Pareto front is generated which is treated as the PF_{approx} . This procedure to generate PF_{approx} is described by Algorithm 1. The notations used in this Algorithm 1 are described in Table 6 for convenience.

Theorem 1 *The proposed methodology converges to the set of optimal PF_{approx} if PF_{known} at iteration $t + 1$ contains only elite solutions from the union of parent and child population from iteration t i.e.,*

$$PF_{known(t+1)} = PF_{known(t)}P_{elite} \cup PF_{known(t)}C_{elite} \\ \implies PF_{known(MaxGen)} < PF_{approx} \quad (11)$$

Where, (11) states that, if the statement “ $PF_{known(t+1)}$ is the union of elite solutions from P_t and C_t of $PF_{known(t)}$ ”

is true then the statement “ PF_{approx} is the succeed of $PF_{known(MaxGen)}$ ” is also true.

Algorithm 1 Proposed methodology.

Input: x_4, k , range of $\{x_1, x_2, x_3, x_5\}$
Output: PF_{approx}

- 1 Set the values of MaxGen and N
- 2 Select P of size N from the set of $\{x_1, x_2, x_3, x_5\}$
- 3 $F1_N = \text{call NSGAI}(P)$
- 4 $F1_S = \text{call SPEA2}(P)$
- 5 $F1_M = \text{call MODEA}(P)$
- 6 Set
 $x = \max\{\text{sizeof}(F1_N), \text{sizeof}(F1_S), \text{sizeof}(F1_M)\}$
- 7 Set $\text{sizeof}(PF_{approx}) = 2 \times x$ and
 $\bar{N} = \text{sizeof}(PF_{approx})$
- 8 $F = F1_N \cup F1_S \cup F1_M$
- 9 $t = 1$
- 10 Set $P_t = F$ // Population at generation
 1
- 11 **while** $t \leq \text{MaxGen}$ **do**
- 12 Apply crossover and mutation on P_t to generate C_t
- 13 $R_t = P_t \cup C_t$
- 14 Apply nondominated sorting on R_t to generate
 PF_j where, $j = 1, \dots, n$ and $n = \text{number of fronts}$
 obtained.
- 15 $j=1$
- 16 **while** $\text{sizeof}(PF_j \cup PF_{j+1}) \leq \bar{N}$ **do**
- 17 $PF_{approx} = PF_j \cup PF_{j+1}$
- 18 $j = j + 1$
- 19 Calculate crowding distance of PF_j
- 20 $y \leftarrow \text{sizeof}(PF_{approx})$
- 21 $PF_{approx} = PF_{approx} \cup PF_j[1 : \bar{N} - y]$
- 22 $P_{t+1} = PF_{approx}$
- 23 $t = t + 1$

Proof In the procedure call $NSGAI(P)$ shown in Table 3, it is shown that, the parent (P_t) and child (C_t) population are combined as $R_t = P_t \cup C_t$ and, is sorted according to nondomination. Thus, at every iteration, all previous and current population members are included in R_t and a comparison is performed among them based on nondomination, which can ensure elitism. Again, the generation of PF_{approx} combines P_t and C_t upon which the nondominated sorting is performed to attain elitism. However, in the procedure $SPEA2(P)$, shown in Table 4 and the procedure $MODEA(P)$, shown in Table 5 do not apply this mechanism to ensure fast convergence. Although an archive (\bar{P}_t) is used in the procedure $SPEA2(P)$ to store the nondominated solutions obtained from current and previous solution at every iteration which ensures elitism. Thus, a fast convergence by the proposed methodology

is obtained as it can attain elitism by $NSGAI(P)$ and $SPEA2(P)$ used here. \square

5.2.1 Computational complexity

The proposed methodology uses three MOEAs such as NSGAI, SPEA2 and MODEA in order to optimize the objective functions discussed earlier. Let us assume, the number of objective functions is M and the population size considered as N. Here, three operations such as fast nondominated sorting, crowding distance assignment and sorting based on crowding distance are involved to determine the computational complexity for NSGAI. The complexity for those operations are obtained as $O(MN^2)$, $O(M(2N)\log(2N))$ and $O(2N\log(2N))$ respectively. Therefore, the worst-case complexity of NSGAI is $O(MN^2)$. The value of M for the problem addressed here is equal to two and the factor N^2 should be preferably reduced, since it leads to long processing time for large population size. The operations involving in SPEA2 for the same purpose pointed out earlier are fitness value assignment, nondominated sorting and truncation operation. Here, the truncation operation requires $O(K^2\log(K))$, where, $K = N + N'$ and N' is the archive size. Hence, the worst-case complexity SPEA2 is $O(K^2\log(K))$. Furthermore, MODEA uses the nondominated sorting and fitness value assignment as in case of NSGAI. Thus, the worst-case time complexity of MODEA becomes $O(MN^2)$.

Finally, an approximate front PF_{approx} is generated from the fronts obtained by NSGAI, SPEA2 and MODEA. In this procedure, nondominated sorting and crowding distance assignment are performed in the same way of NSGAI which makes the worst-case complexity of generating PF_{approx} is $O(MN^2)$. Hence, the overall computational complexity for the proposed methodology is determined as $O(MN^2 + K^2\log(K))$.

6 Performance measure

There are several metrics to assess the performance of MOEAs [47]. Such performance assessment depends on the evaluation of convergence and diversity of the MOEAs. Here, convergence defines the closeness of the resultant nondominated front of the algorithms to the true Pareto front, while diversity indicates the distribution of the solutions along the Pareto front. Few of those metrics used in several existing works are not sufficient enough to determine the best algorithm. Hence, to detail out the performance evaluation for the proposed work, the following six metrics are used for each of the three MOEAs mentioned earlier. These metrics are introduced herewith for ease of further discussions.

Table 5 MODEA pseudocode

MODEA(P)
<p>Begin MODEA</p> <p>Input : A random population (X) of size N_p.</p> <p>Output : X.</p> <p>Calculate fitness function of X_i for each $i = 1$ to N_p</p> <p>Perform nondominated sorting on X to discard dominated solutions.</p> <p>while maximum generation not reached</p> <p> for $i = 1$ to (size of X)</p> <p> Apply trigonometric mutation operation on X_i to generate V_i</p> <p> Set $p_i = rand(0, 1)$;</p> <p> if $p_i \leq$ crossover rate</p> <p> $Y_i \leftarrow V_i$</p> <p> else</p> <p> $Y_i \leftarrow X_i$</p> <p> end if</p> <p> end for</p> <p> Calculate fitness function of X_i and Y_i</p> <p> for $i = 1$ to (size of X)</p> <p> if Y_i dominates X_i</p> <p> $X_i \leftarrow Y_i$</p> <p> else if X_i dominates Y_i</p> <p> discard Y_i</p> <p> else</p> <p> Replace X_j for which Y_i dominates X_j</p> <p> end if</p> <p> end for</p> <p>end while</p> <p>End MODEA</p>

6.1 Generational distance (GD)

GD [48] is used to measure the closeness of the nondominated solutions with respect to true Pareto front. Hence, it is evaluated to assess the convergence of the solutions by the given expression:

$$GD = \frac{\sqrt{\sum_{i=1}^x d_i^2}}{x} \quad (12)$$

Where, 'x' represents the number of solutions in the nondominated front and ' d_i ' denotes the distance of every solution (i) in the nondominated front to its nearest solution in the true Pareto front. The smaller value of GD specifies the better convergence of the algorithm [12].

6.2 Inverted generational distance (IGD)

Unlike GD, IGD [48] measures the distance of each element in the true Pareto front to the nearest element in the nondominated front. Thus, it can measure the convergence as well as the diversity of the algorithm because of

the endpoints in the true Pareto front. Hence, IGD can be determined as follows:

$$IGD = \frac{\sum_{v \in PF} d(v, S_N)}{|PF|} \quad (13)$$

Where, S_N and PF are the set of solutions in the nondominated front and the Pareto front respectively. The term $d(v, S_N)$ in (13) denotes the distance of the solutions v

Table 6 Notations used in Algorithm 1

Notations	Description
$MaxGen$	Maximum generation
PF_{approx}	Approximate front
$F1_N$	First nondominated front from NSGAI1
$F1_S$	First nondominated front from SPEA2
$F1_M$	First nondominated front from MODEA
P_t	Population at generation t
C_t	Child at generation t
PF_j	j^{th} nondominated front of PF_{approx}

in PF to the nearest element in S_N . Hence, a smaller value of IGD signifies better diversity.

6.3 Space

Space [49] is a measure of how uniformly the solutions are distributed throughout the nondominated front. Thus, it measures the diversity of the solution. Space is calculated as follows:

$$Space = \sqrt{\frac{1}{x} \sum_{i=1}^x (d_i - \bar{d})^2} \tag{14}$$

Here, d_i denotes the same as discussed for GD, ‘ x ’ is the number of solutions in the nondominated front and ‘ \bar{d} ’ represents the average of all the distances d_i . A smaller value of this metric signifies better distribution of the solutions along the resultant front. Therefore, a space value of zero implies that the solutions are equally distributed.

6.4 Spread (Δ)

Spread [41] measures the diversity of the nondominated solutions. In order to calculate spread, the nondominated front is initially extended by fitting a curve parallel to the true Pareto front. Therefore, two extreme points are assumed at the end of the nondominated front. Hence, the metric Δ can be formulated as follows:

$$\Delta = \frac{d_f + d_l + \sum_{i=1}^{x-1} |d_i - \bar{d}|}{d_f + d_l + (x - 1)\bar{d}} \tag{15}$$

Here, ‘ d_f ’ and ‘ d_l ’ are the distances from two extreme points to the first and last points of the nondominated front respectively. The term \bar{d} in (15) is the average of all the distances d_i , where d_i represents the distance between two consecutive solutions and x denotes the number of solutions on the nondominated front.

Different values of Δ imply various conditions. The value of Δ can be zero if all the points are equally distributed along with $d_f = d_l = 0$ i.e., the nondominated front is widely spread. However, for a large variance of d_i , d_f and d_l , Δ can hold a value greater than one.

6.5 Hypervolume (HV)

HV [50] determines the area covered by all the solutions in the nondominated front to a reference point r . It is formulated by the union of the rectangular area from r to the solutions of the nondominated front [12] as:

$$HV = \bigcup_{i=1}^x a_i \tag{16}$$

In (16), a_i is the area of the rectangles from the reference point r to the solutions in the nondominated front and x is the number of solutions on the nondominated front.

6.6 Maximum Pareto front error (MPFE)

MPFE [51] is a measurement of the error i.e., the distance between nondominated front and true Pareto front. It is formulated as:

$$MPFE = \max(d_i) \tag{17}$$

Where, d_i in (17) denotes the same as discussed in GD. Hence, MPFE measures the largest minimum distance from all the solutions of nondominated front to the true Pareto front. A smaller value of MPFE indicates better performance of the algorithm.

7 Simulation studies

7.1 Simulation setup

The proposed street lighting framework is designed with several parameters associated with street conditions and the values of these parameters used in the simulation follow the recommendation by the CIE. Here, each individual of the population consists of a set of combination of the lighting parameters $\{x_1, x_2, x_3, x_5\}$. Here, the values of the parameters for a single instance are kept as equal in case of the three MOEAs used in the proposed work. For SPEA2, the binary tournament is used for selection operation, and in case of NSGAI and MODEA, nondominated sorting serves the purpose of the selection process. Some other essential parameters related to MOEA are the number of generations, population size, crossover rate, mutation rate etc. The archive size in SPEA2 is considered to be the same as the population size. The parameters, along with their values used in the simulation, are shown in Table 7.

Table 7 Parameters used in simulation

Parameters	Value
Number of decision variables $\{x_1, x_2, x_3, x_5\}$	4
Maximum number of generation in MOEA	100
Population Size	50
Archive size in SPEA2	50
Crossover rate	0.7
Mutation rate	0.02

7.2 Dataset used in MOEAs

In the proposed work, the system considers the values of E_{av} and k as a set of input parameters $\{x_4, k\}$. Here, E_{av} depends on the lighting class provided by the user. It is to be noted here that, in case of M lighting class, the calculation is based on L_{av} . The unit of L_{av} is *candela/m²*, whereas, the unit of D_p is $W/(lx.m^2)$. Hence, the values of L_{av} is converted to E_{av} i.e., the unit *candela* is converted to the unit *lx* for the development of M lighting class. Initially, the MOEAs generate a set of random population where, every individual of the population comprises with a set of combination of the lighting parameters $\{x_1, x_2, x_3, x_5\}$ as discussed earlier. The data sets used in the simulation of MOEAs are presented in Table 8.

7.3 Simulation results

7.3.1 Instance setting and its evaluation

Till now, existing works have focused on the design of street lighting by tuning the parameters involved in this system. However, as per our best knowledge, the performance of several lighting subclasses, and the consideration of installation design factor are not yet discussed under a single platform. Here, for measuring the performance of the proposed work, several instances are presented which include the lighting classes and its corresponding values of E_{av} as well as the values of k . For example, one instance is considered as “30C2”. Here, the first number i.e., “30” represents the value of E_{av} , the letter “C” represents lighting class and last number “2” signifies the design of *two-sided* installation for $k = 2$. Hence, by 30C2, it indicates the installation of *C1* lighting class in a *two-sided* configuration with $E_{av} = 30lx$. In the proposed work, 15 instances are evaluated by NSGAI, SPEA2 and MODEA. For ease of understanding, suitable solutions of those 15 instances performed by NSGAI are

discussed in Table 9. Similarly, the solutions from SPEA2 and MODEA can be obtained. Each instance is evaluated with 15 independent runs. The nondominated front ($F1$) of the instances “7.5P1” and “30C2” along with the approximate front (PF_{approx}) for one independent run are shown in Fig. 5.

From Fig. 5a, it is evident that, the value of D_p is 0.01 for $U_0 = 0.2$. Similarly, D_p has value 0.01 for $U_0 = 0.4$ as shown in Fig. 5b. Hence, the lighting of these two instances can be installed with energy class A as per Table 1. Again, as discussed earlier, the minimum values of U_0 for class P and C are 0.20 and 0.40, respectively, so, the solutions having U_0 lesser than these values are discarded from the obtained solutions.

7.3.2 Statistical Analysis

The outcomes of proposed MOEA based models are analysed in accordance with the performance metrics introduced earlier. Here, for presenting with detail, the results with respect to performance metrics are empirically analysed for two central tendency measures such as mean and median, along with two variability measures such as standard deviation (SD) and interquartile range (IQR) [52]. Here, the evaluation of mean, median, SD and IQR are performed after 15 independent runs on each of the 15 instances mentioned in Table 9. From Table 9, it can be stated that the values of the objective functions D_p and U_0 remain close with the perturbation of the decision variable. Hence, it produces robustness of the Pareto front solutions. In order to compare different MOEAs used in the proposed framework, the plots related to mean, median, SD and IQR of GD, IGD, space, spread, HV and MPFE of all the instances for NSGAI, SPEA2 and MODEA are shown in Figs. 6, 7, 8, 9, 10, and 11. An ANOVA test is also performed at significance level $\alpha = 0.05$ on 15 instances for each of the performance metrics to show the variation of the outcomes from three different MOEAs. The summaries of

Table 8 Data set used in MOEAs

Variables	Values	Description	Unit
x_1	10-50	Inter-distance (S) between two luminaries	meter(m)
x_2	6-10	Height (H) of the luminari	meter(m)
x_3	6-10	Width (ω) of the road	meter(m)
x_4	1.0, 2.0, 7.5, 10, 15, 20, 30, 50	Average of illuminance or luminance (E_{av} or L_{av})	(lx) or (<i>candela/m²</i>)
x_5	15-100	Power supply (P) of the luminari	watt(W)
k	1, 2	one-sided and two-sided installation design	NA

Table 9 Solutions obtained for 15 instances using NSGAI

Instances	Lighting subclass	Installation Design factor (k)	Solutions $\{x_1, x_2, x_3, x_5\}$	D_p	U_0
30C2	C1	2	{30.5268, 6.0356, 8.0199, 51.7612}	0.0142	0.5067
30C1	C1	1	{17.9278, 7.9999, 6.0306, 50.8258}	0.0157	0.6507
15P1	P1	1	{32.4539, 7.1011, 6.1838, 49.4989}	0.0164	0.4981
15P2	P1	2	{49.9999, 6.1560, 8.6916, 48.2591}	0.0148	0.2001
50C2	C0	2	{14.9274, 8.8845, 10.000, 55.2017}	0.0147	0.8745
50C1	C0	1	{10.200, 9.0152, 6.0013, 82.3229}	0.0269	0.8957
2.0P1	P6	1	{49.1920, 8.5990, 7.4268, 18.0125}	0.0246	0.2600
2.0M1	M1	1	{17.1022, 8.9999, 6.0175, 50.7375}	0.0229	0.6772
20C1	C2	1	{20.6244, 7.9890, 6.0224, 51.2901}	0.0207	0.7661
20C2	C2	2	{32.3184, 7.1288, 8.9801, 50.8340}	0.0175	0.7018
1.0M2	M3	2	{31.6341, 6.6372, 9.8697, 40.4714}	0.0240	0.7035
10C1	C4	1	{45.4471, 8.0344, 6.1122, 50.9523}	0.0183	0.4157
10C2	C4	2	{49.5281, 7.3539, 9.9802, 51.0252}	0.0206	0.7813
7.5P1	P3	1	{45.4131, 9.0992, 6.9790, 50.8924}	0.0214	0.2527
7.5P2	P3	2	{48.2880, 7.5783, 9.5217, 41.2667}	0.0239	0.3186

ANOVA test and its corresponding box plots are presented in Table 10 and in Fig. 12 respectively.

From Fig. 6, it is stated that, GD holds different values for different MOEAs. For some of the instances, one algorithm performs the best, while the same algorithm performs the worst for others. For example, NSGAI performs better in the case of 15P2, while for 7.5P2 the performance of MODEA is better over NSGAI and SPEA2. Hence, to compare the performance of GD, the box plots are analysed, as shown in Fig. 12a. From this Fig. 12a, it is revealed that, both NSGAI and SPEA2 perform well in the case of GD than MODEA. Since GD determines the closeness to the Pareto front, therefore, the algorithms NSGAI and SPEA2

can be treated as equally converged to the Pareto front while MODEA is less converged than the other two.

It is already discussed that, the diversity of the MOEA algorithms is measured by the performance metrics IGD, spread and HV. It is shown in Figs. 7, 9 and 10, the performance of NSGAI is better than SPEA2 and MODEA. The box plots of IGD, spread and HV, shown in Fig. 12b, d and e respectively also indicate the same. Although space is used to determine the diversity, however, it only measures the distribution of the solutions. The distance from the extreme two points of the Pareto front is not calculated in space. Like GD, the value of the metric space as shown in Fig. 8 varies in case of some instances for different

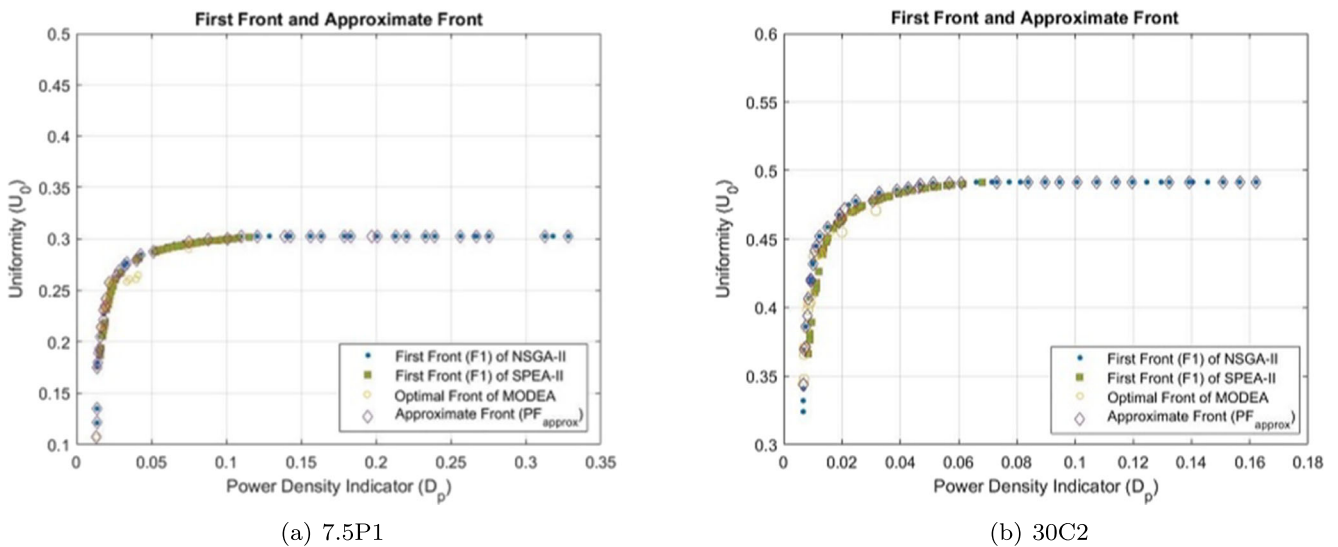


Fig. 5 Evaluation of the proposed model (a) 7.5P1 and (b) 30C2

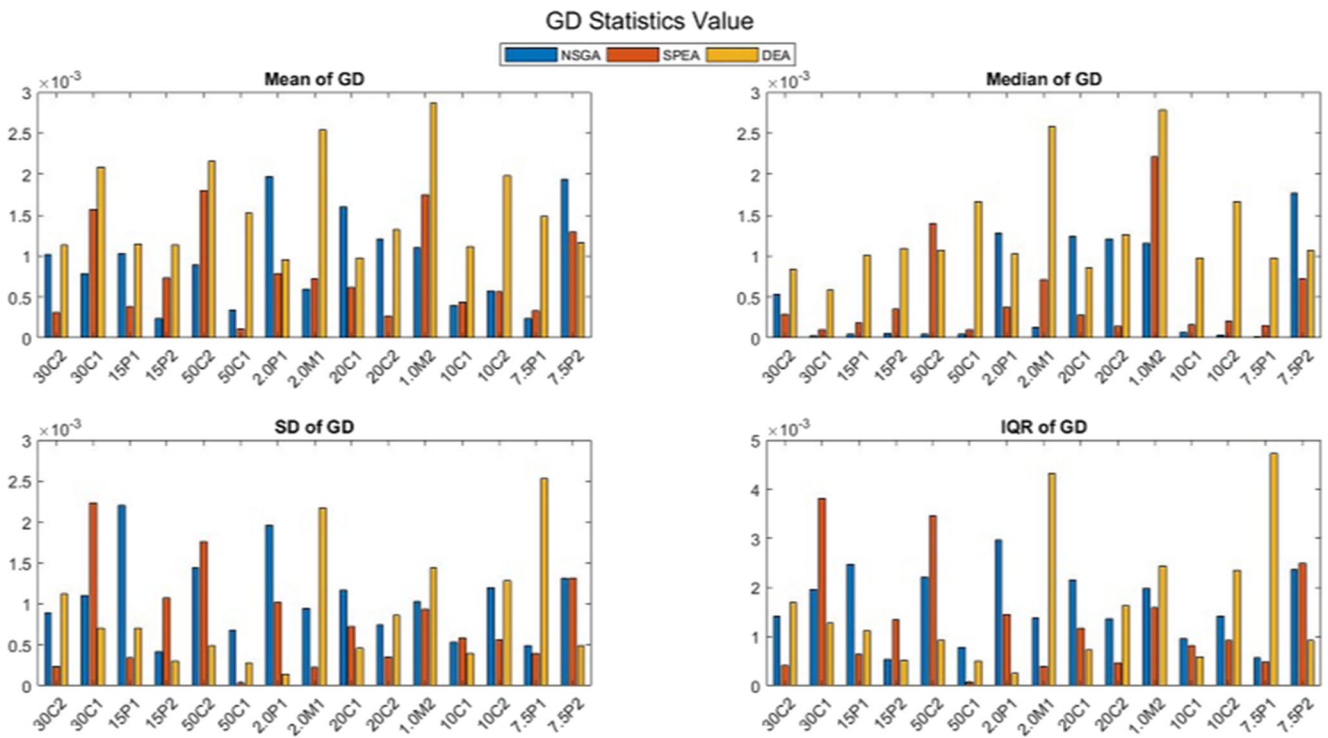


Fig. 6 Mean, median, SD and IQR of GD for NSGAII, SPEA2 and MODEA

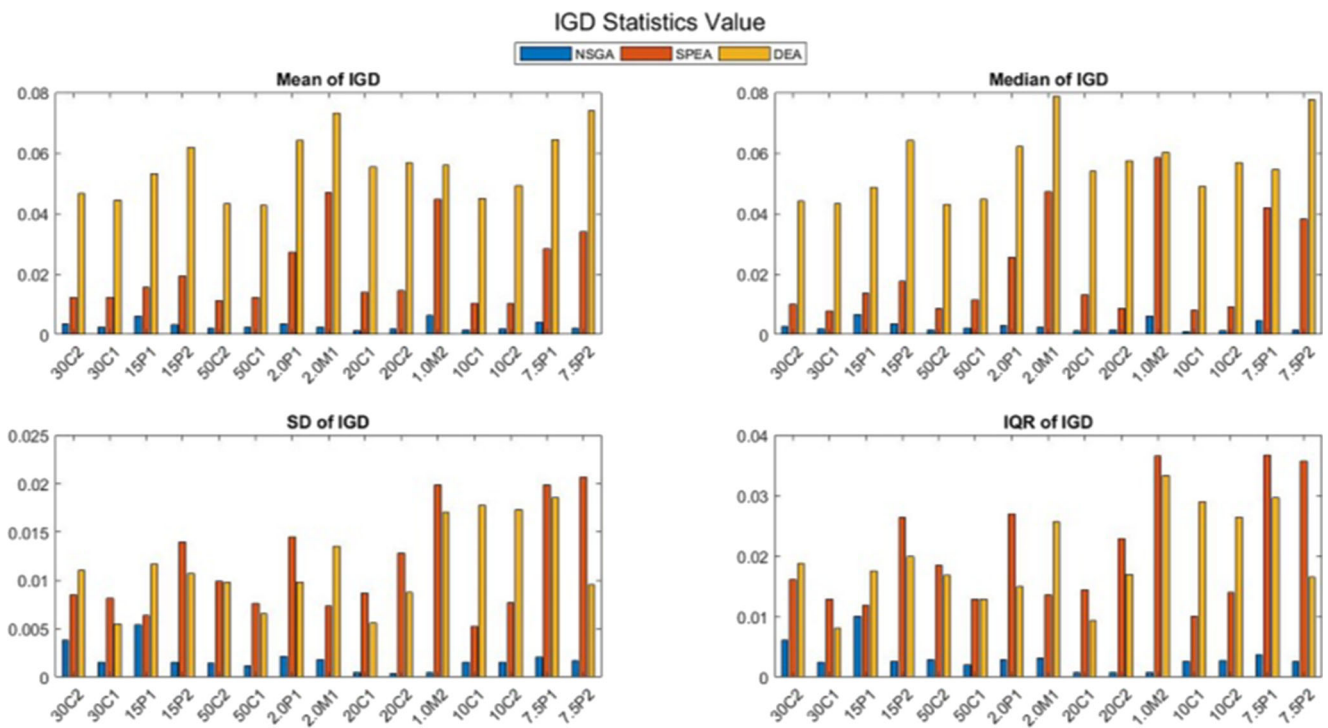


Fig. 7 Mean, median, SD and IQR of IGD for NSGAII, SPEA2 and MODEA

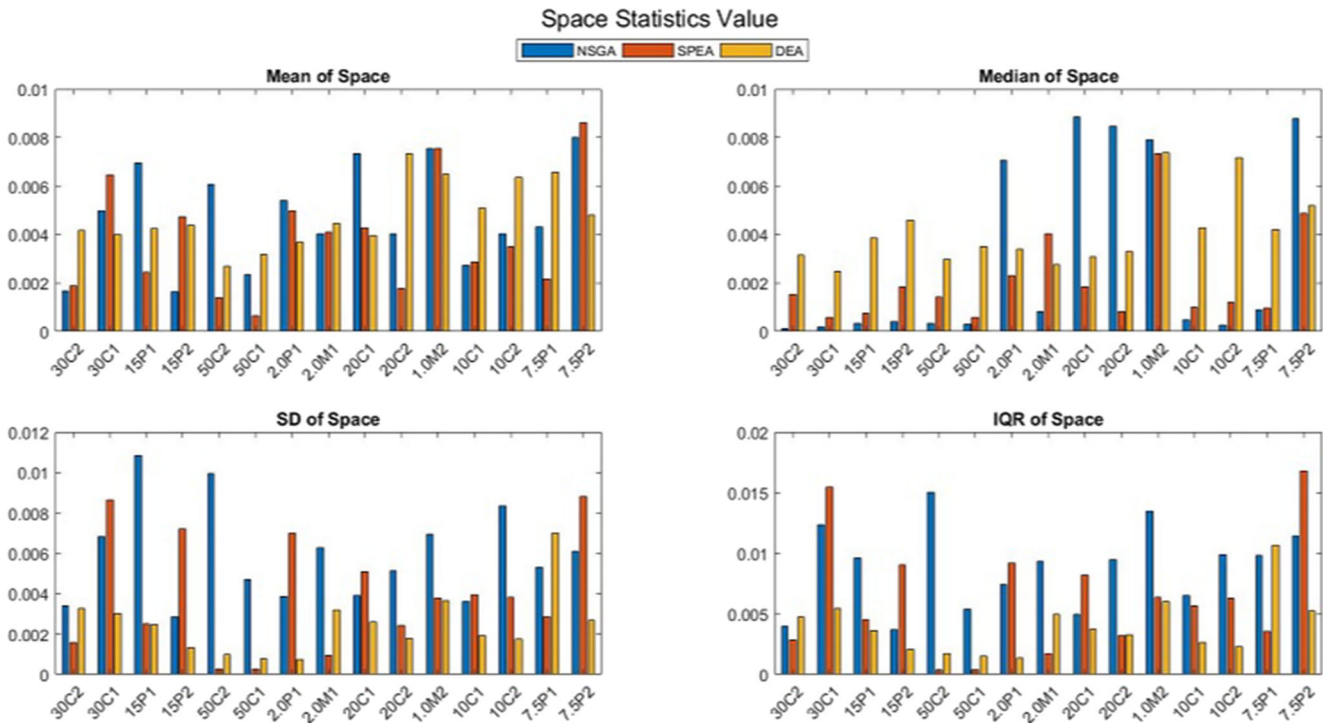


Fig. 8 Mean, median, SD and IQR of space for NSGAI, SPEA2 and MODEA

MOEAs. Hence, Fig. 12c is referred to analyse this metric for the three MOEAs. Fig. 12c reflects that the value of space in case of SPEA2 is less than others revealing that the solutions of SPEA2 are well distributed. However, it is not

well diverse than NSGAI, as the value of spread is less in case of NSGAI as shown in Fig. 12d. Hence, the solutions obtained by NSGAI can be treated as well diverse than those of SPEA2 and MODEA.

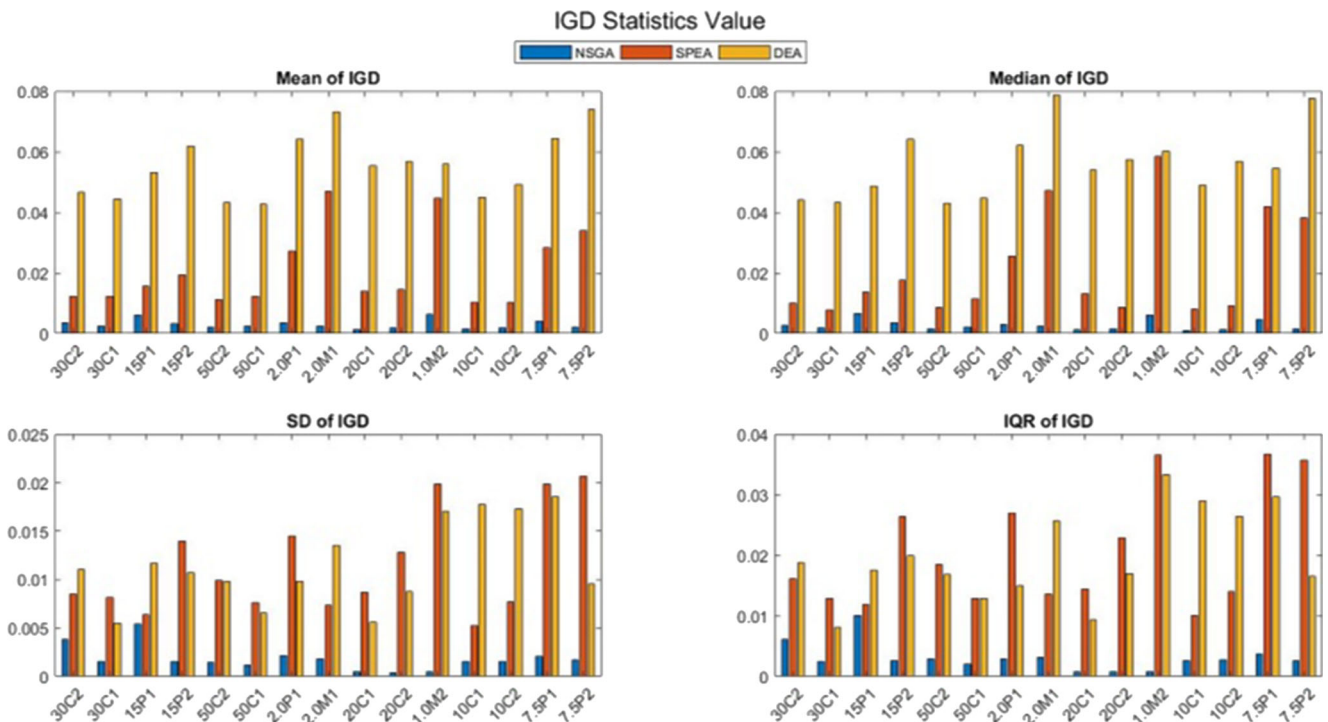


Fig. 9 Mean, median, SD and IQR of spread for NSGAI, SPEA2 and MODEA

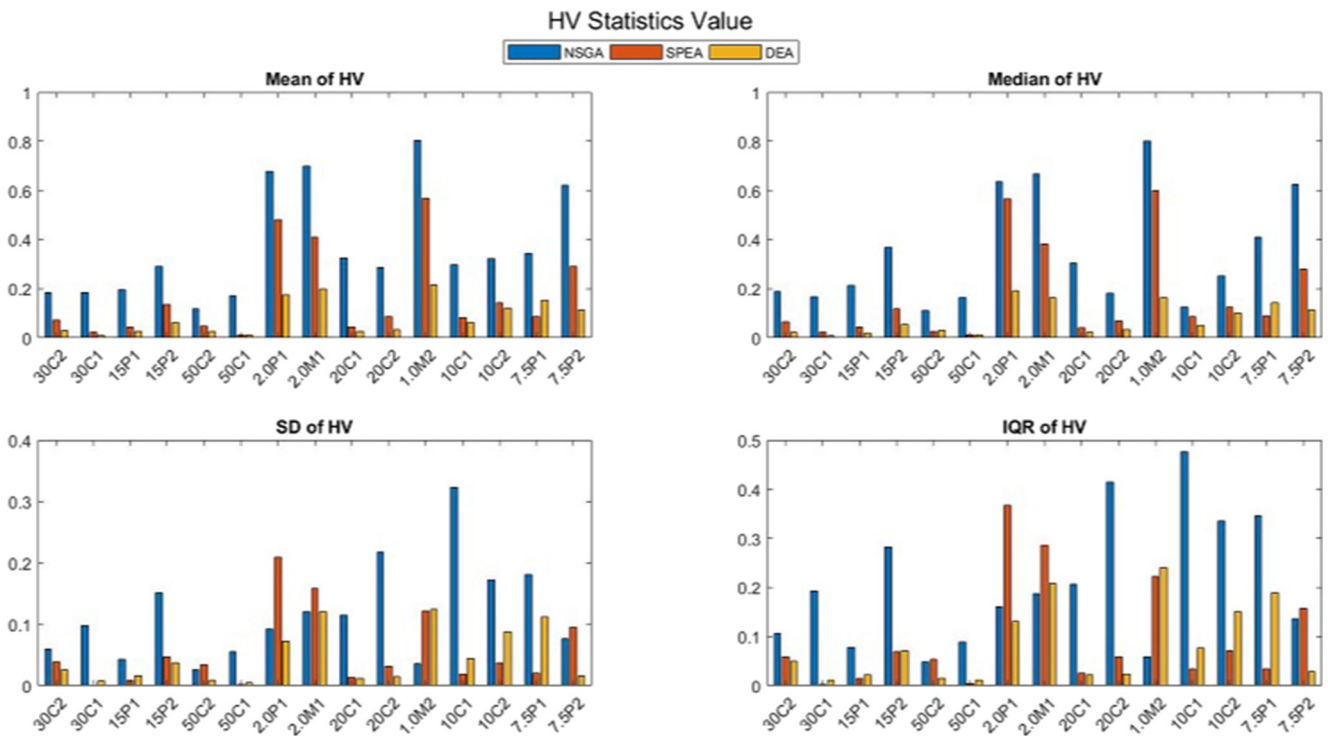


Fig. 10 Mean, median, SD and IQR of HV for NSGAI, SPEA2 and MODEA

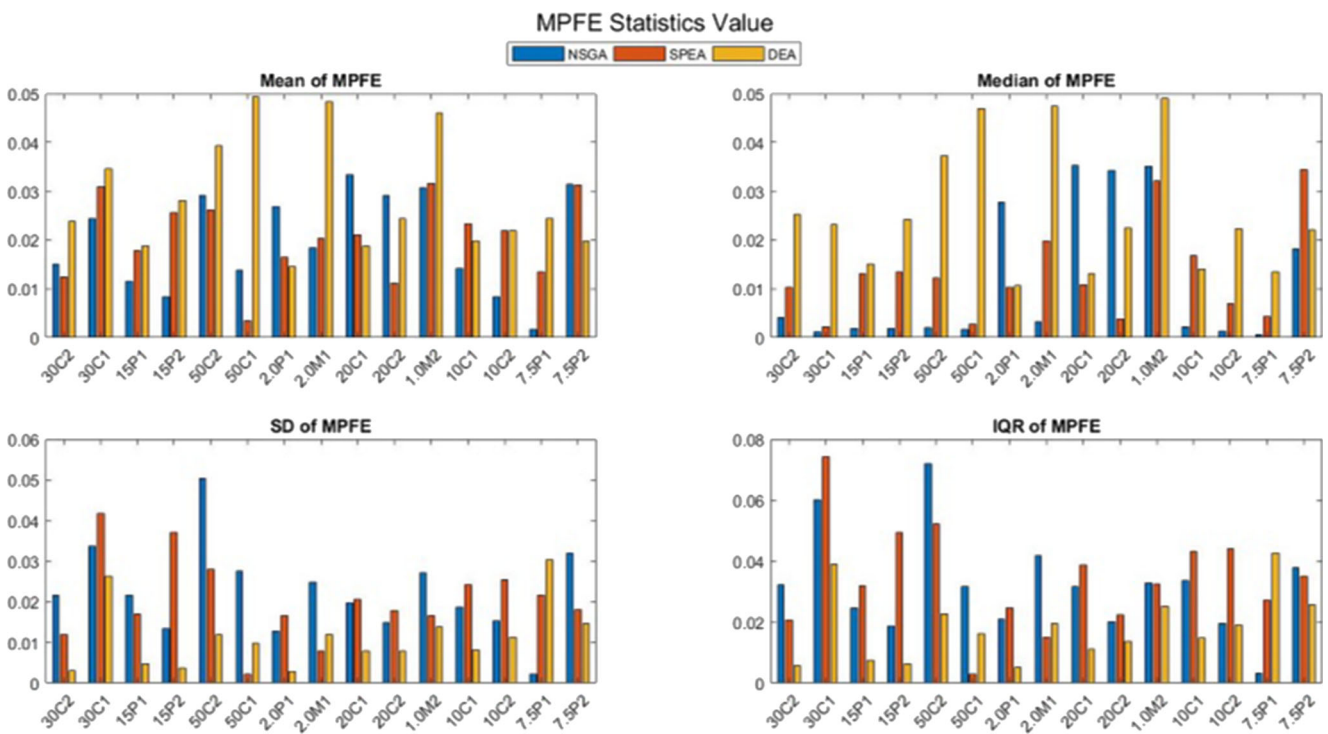


Fig. 11 Mean, median, SD and IQR of MPFE for NSGAI, SPEA2 and MODEA

Table 10 ANOVA test summaries

Critical value (at $\alpha = 0.05$) = 3.220

Degree of freedom = 2,42

Performance metrics	(Mean - x_i) ²	SSQ_b	F-ratio	Remarks
GD	NSGAI2 = 4.519E-06, SPEA2 = 4.3423E-06, MODEA = 5.145E-06	5.319E-06	7.975	Since 7.975 > 3.220, the results are significant at the 5% significance level.
IGD	NSGAI2 = 3.168E-05, SPEA2 = 0.00216886, MODEA = 0.0015099	0.02122	120.131	Since 120.131 > 3.220, the results are significant at the 5% significance level.
Space	NSGAI2 = 6.319E-05, SPEA2 = 7.5776E-05, MODEA = 2.545E-05	8.613E-06	1.099	Since 1.099 < 3.220, the results are not significantly different for 3 groups at the 5% significance level.
Spread	NSGAI2 = 0.081276228, SPEA2 = 0.242111952, MODEA = 0.117184596	5.435413	259.080	Since 259.080 > 3.220, the results are significant at the 5% significance level.
HV	NSGAI2 = 0.681095673, SPEA2 = 0.454625946, MODEA = 0.074124876	0.637366	11.063	Since 11.063 > 3.220, hence, the results are significant at the 5% significance level.
MPFE	NSGAI2 = 0.001440957, SPEA2 = 0.000933551, MODEA = 0.001929699	0.000761	3.713	Since 3.713 > 3.220, the results are different for 3 groups at the 5% significance level.

The metric MPFE works similar as GD for all these three MOEAs as shown in Fig. 11. To compare the errors in the proposed algorithms, the box plot is shown in Fig. 12f. Like GD, for MPFE, the performance of NSGAI2 and SPEA2 is better than those for MODEA.

Another analysis is also performed to show the variations of performance metrics in accordance of different size of datasets such as small, medium and large. Here, the small data size considers 6 instances for the all the subclasses of P lighting class by considering $k = 1$. Similarly, the

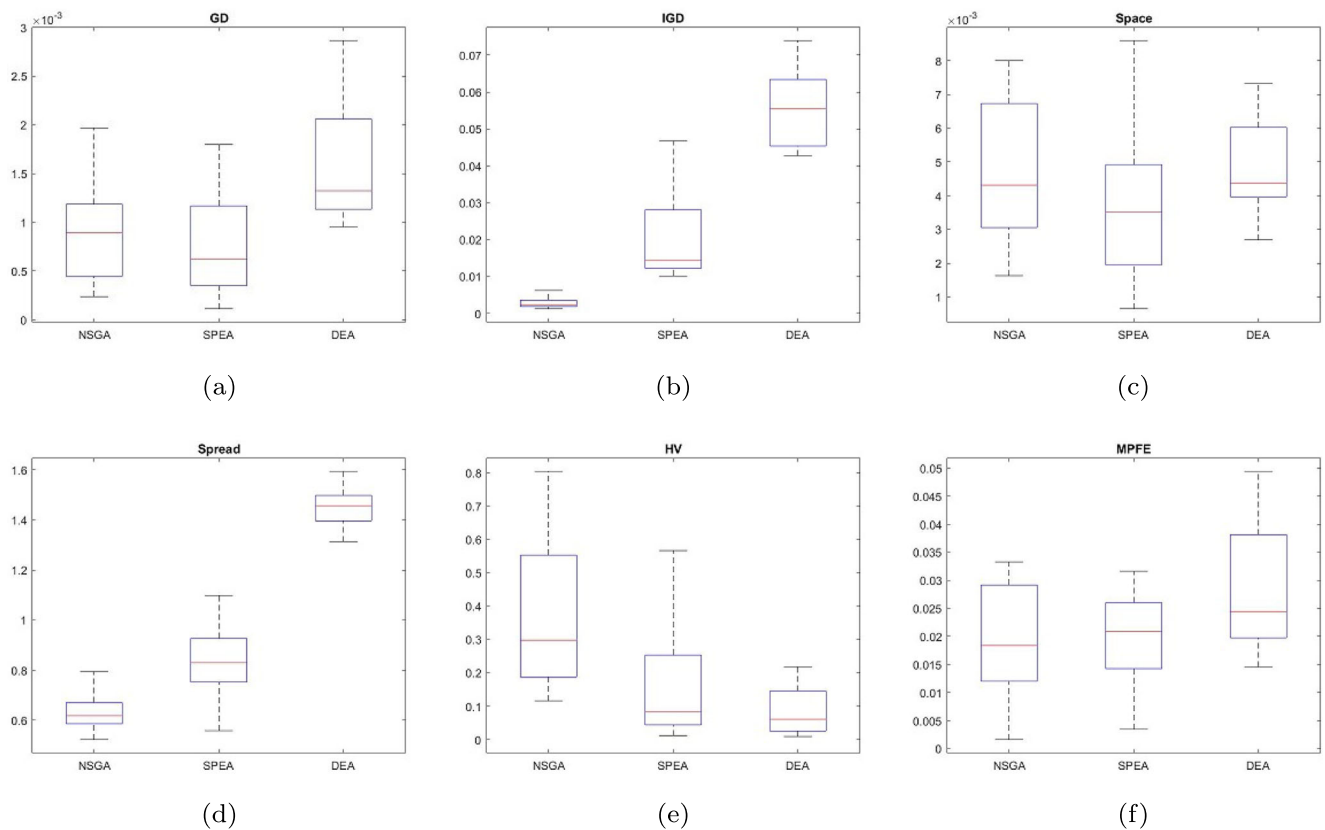


Fig. 12 Box plot of the performance metrics with respect to NSGAI2, SPEA2 and MODEA

large data sizes consider all the subclasses of P, C and M lighting class with consideration of both $k = 1$ and $k = 2$. Thus, the large data size consists of 36 lighting instances, whereas, the medium data size consists of the 15 instances as evident from CIE recommendation. The analysis of these three types of data sizes for the performance metrics i.e., GD, IGD, space, spread, HV and MPFE are shown in Fig. 13. It can be observed from Fig. 13b, d and e that, the metrics IGD, spread and HV perform better for NSGAII than SPEA2 and these three metrics have worst performance for MODEA. Hence, it can be said that, NSGAII is more diverse than SPEA2 while SPEA2 is more diverse than MODEA. However, Fig. 13c shows the value of space is less for SPEA2 than NSGAII which implies that the solutions are well distributed in case of SPEA2. For other two metrics shown in Fig. 13a and f, i.e., GD and MPFE, for some of the instances, the performance of NSGAII is better while for others SPEA2 performs better than NSGAII. Again, for both the metrics, the performance of MODEA is not better than the other two. It can be observed that, the overall performance of the proposed methodology on various performance metrics remains the same for different data sizes, which indicates the scalability of the outcomes from the proposed model.

For the ANOVA test, each of the 15 instances is analysed with three groups as NSGAII, SPEA2 and DEA for all the performance metrics. Hence, the test is consisted of 45 samples. The sum of square between groups (SSQ_b) as well as the sum of square of three different groups ($(Mean - x_i)^2$) are presented in Table 10. In this table, the F-ratio determines the variation of the outcomes from the MOEAs in terms of different performance metrics. Here, in case of IGD and spread, the F-ratio is significantly more than the critical value at $F(2,42)$, i.e., 3.220. This implies that, there is a variation in the outcomes of NSGAII, SPEA2 and MODEA for these two performance metrics. The same reflects in the box plots of these two metrics as shown in Fig. 12b and d. Whereas, in case of space, the F-ratio is less than critical value implying, the outcomes are not significant for three MOEAs. In other performance metrics such as GD, HV and MPFE, the F-ratio is greater than the critical value, indicating that the results of the three MOEAs are significant at $\alpha = 0.05$ significance level.

From this detailed analysis, it is clear that, NSGAII performs better than SPEA2 and MODEA for IGD, HV and spread, while in case of space, the performance of SPEA2 is better than MODEA and in this similar context, MODEA performs better than NSGAII. For GD and MPFE, NSGAII

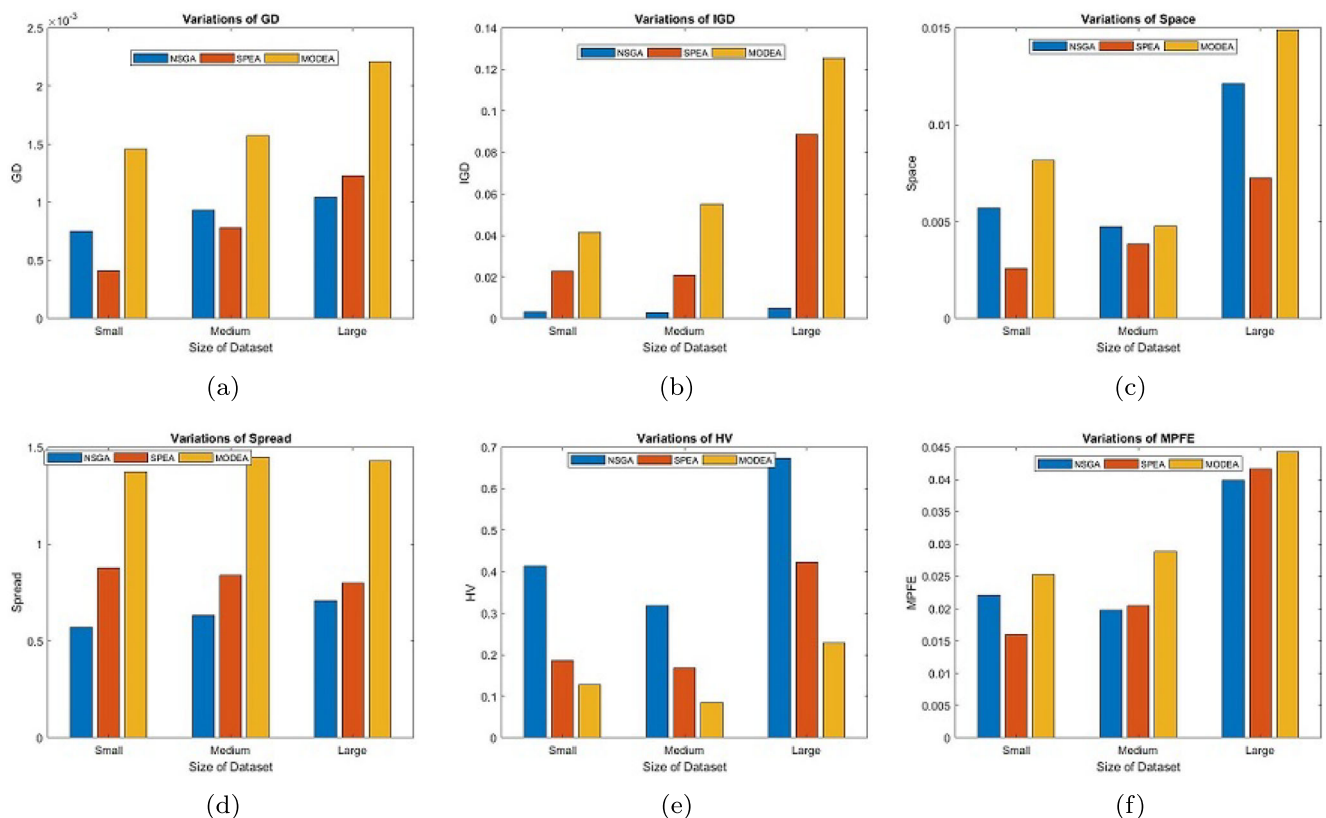


Fig. 13 Variations of performance metrics in accordance of different size of datasets with respect to NSGAII, SPEA2 and MODEA

and SPEA2 both have an equal performance over MODEA. Hence, it can be stated that, NSGAI is well diverse than the others, although MODEA and SPEA2 have more equally distributed solutions, while SPEA2 and NSGAI can be treated as equally converged. Thus, the values of these performance metrics under statistical analysis indicate the closeness of the solutions obtained from the proposed MOEAs, to the PF_{approx} . Hence, it is stated that the Pareto optimal solutions for ϵ and U_0 obtained by different MOEAs can be very much effective.

7.3.3 Validation and comparison of results

For performance evaluation of the proposed street lighting framework, it is essential to validate the simulation results i.e., whether it satisfies the recommendation of CIE or not. Here, the outcomes of the proposed algorithm are compared with DIALux. For the validation in DIALux, EN 13201:2015 standard is used. Although DIALux provides the values of the parameters that are used for the installation of the lighting system, however, it cannot determine satisfactory results for measuring the efficiency of the system.

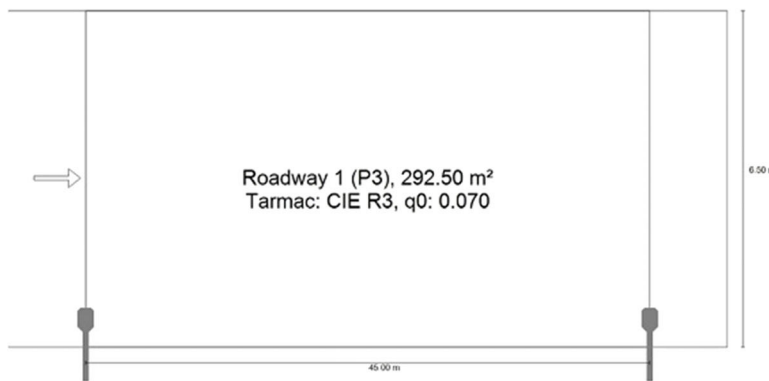
Hence, it is necessary to use MOEAs with the combination of the design parameters related to the street lights that can maximize the ϵ and U_0 of the system.

Finally, the results of those MOEAs are compared with DIALux. Here, the detailed reports of the software validation for the instances 7.5P1 and 30C2 are shown in Figs. 14 and 15. The Figs. 14 and 15 show the results of both D_p and U_0 as highlighted in green colour.

For completeness of the proposed work, the solutions obtained for those 15 instances mentioned earlier are compared with DIALux and the values of each parameter related to the installation are shown in Table 11. However, DIALux fails to provide the U_0 values in case of P lighting class which are mentioned as not applicable (NA) in Table 11, although it can be determined by the values of E_{av} and minimum illuminance. For every instance, the solutions i.e., luminari spacing, height of luminaries, road width and power requirement of the installation are compared with DIALux results. Here, the values of the installation parameters for obtaining an efficient lighting system closely match with the solutions obtained by DIALux. For example, the values of S, H, ω, P, D_p and U_0 in case of 30C2

7.5P1 - Alternative 7

Summary (according to EN 13201:2015)



Article name	URBA L 48L35 RC ANT BP CL1 10M MTP76 L74 [STD]	$\Phi_{luminaire}$	7953 lm
		η	100.00 %
Fitting	1x LED 51 W		

URBA L 48L35 RC ANT BP CL1 10M MTP76 L74 [STD] (single side bottom)	
Pole distance	45.000 m
(1) Light spot height	8.000 m
(2) Light point overhang	0.500 m
(3) Boom inclination	5.0°
(4) Boom length	0.500 m
Annual operating hours	4000 h: 100.0 %, 51.0 W

Results for valuation fields

	Symbol	Calculated	Target	Check
Roadway 1 (P3)	E_{av}	8.95 lx	[7.50 - 11.25] lx	✓
	E_{min}	1.50 lx	≥ 1.50 lx	✓

A maintenance factor of 0.67 was used for calculating for the installation

Results for energy efficiency indicators

	Symbol	Calculated	Consumption
7.5P1	D_p	0.019 W/lx*m²	-
URBA L 48L35 RC ANT BP CL1 10M MTP76 L74 [STD] (single side bottom)	D_e	0.7 kWh/m²*yr	204.0 kWh/yr

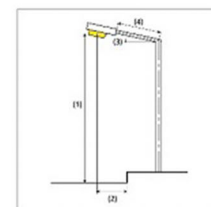


Fig. 14 Screen shot of DIALux based solution for instance 7.5P1

30C2 · Alternative 9

Summary (according to EN 13201:2015)

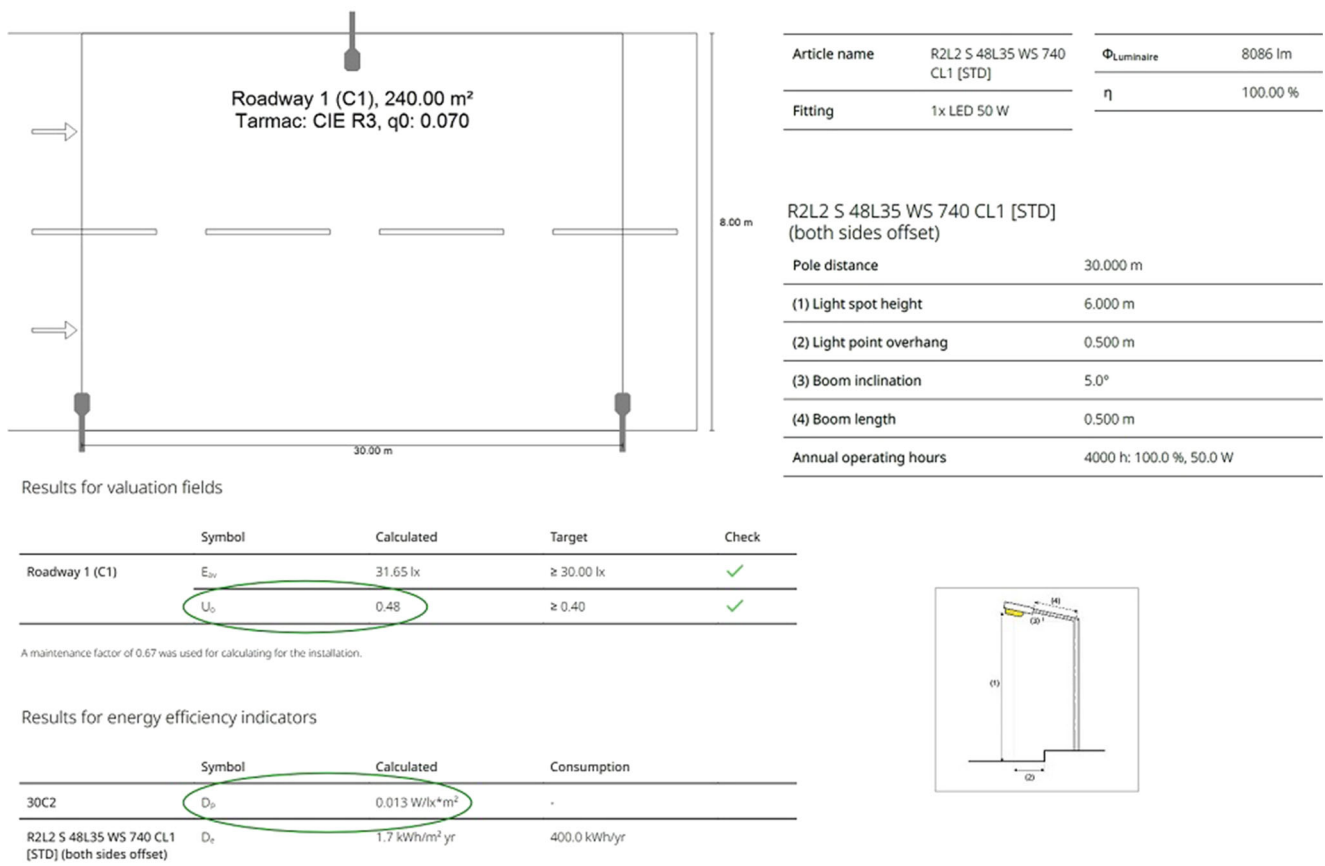


Fig. 15 Screen shot of DIALux based solution for instance 30C2

as shown in Fig. 15 are 30.00, 6.00, 8.00, 50, 0.013 and 0.48 respectively whereas the corresponding values of these parameters obtained from the proposed algorithm are 30.5268, 6.0356, 8.0199, 51, 7612, 0.0140 and 0.5067 respectively, as shown in Table 11. Similarly, in case of 7.5P1, the values of these parameters for proposed algorithm and DIALux are 45.4131, 9.0992, 6.9790, 50.8924, 0.0214, 0.2527 and 45.00, 8.00, 6.50, 51, 0.019, NA respectively, as shown in Table 11 and Fig. 14. So, a good attainment model for obtaining energy efficient lighting is discussed by the proposed work.

7.3.4 Comparison over existing approaches

The better performance of the proposed methodology over existing approaches is highlighted on different aspects of energy in street lighting system as discussed next.

- *Comparison on energy efficiency:*
The energy efficiency of the street lighting system is obtained from various energy classes discussed earlier

that holds different values of D_p . Hence, the value of D_p resulted from the proposed methodology is compared with some existing approaches [6, 15, 16]. These comparisons are shown in Table 12. From this table, it can be said that, the values of D_p are minimized in the proposed methodology over existing algorithms. In some cases, the values of U_0 can violate the recommendation from the standardization which are shown by red cross mark in the table. Again, the objective of the proposed work is to design an energy efficient street lighting system by minimizing D_p and maximizing U_0 by applying MOEA. Hence, it can be said that, the nondominated front obtained from the proposed methodology are closer to the approximate front than that of the existing works. Therefore, the proposed methodology can be mentioned as more converged than the existing algorithms which in turn indicates that the proposed work can attain an improved energy class over [6, 15, 16].

- *Comparison on power of the luminaire:*

Table 11 Comparison between NSGAI solutions obtained for the proposed work and DIALux

Instance	Model	Lighting class	E_{av}	k	S	H	ω	P	D_p	U_0	Energy class
30C2	Proposed	C1	30	2	30.526	6.0356	8.0199	51.7612	0.0140	0.5067	A
	DIALux	C1	31.65	2	30.00	6.00	8.00	50	0.013	0.48	A
30C1	Proposed	C1	30	1	17.927	7.9999	6.0306	50.8258	0.0157	0.6507	B
	DIALux	C1	30.04	1	18.00	6.00	6.00	50	0.015	0.65	B
15P1	Proposed	P1	15	1	32.453	7.1011	6.1838	49.4989	0.0164	0.4981	B
	DIALux	P1	15.45	1	30.00	7.00	6.00	51	0.018	NA	B
15P2	Proposed	P2	15	2	49.999	6.1560	8.6919	48.2591	0.0148	0.2001	A
	DIALux	P2	17.74	2	50.00	6.500	8.00	50	0.014	NA	A
50C2	Proposed	C0	50	2	14.927	8.8845	10.000	55.2017	0.0147	0.8745	A
	DIALux	C0	51.44	2	13.00	8.00	9.50	55	0.017	0.85	B
50C1	Proposed	C0	50	1	10.200	9.0152	6.0013	82.3229	0.0269	0.8957	C
	DIALux	C0	50.32	1	10.00	9.00	6.00	81	0.027	0.89	C
2.0P1	Proposed	P6	2.0	1	49.192	8.5990	7.4268	18.0125	0.0246	0.2600	B
	DIALux	P6	2.95	1	48.00	8.00	7.00	20	0.020	NA	B
2.0M1	Proposed	M1	2.0	1	17.102	8.9999	6.0175	50.7375	0.0229	0.6772	B
	DIALux	M1	2.15	1	17.00	8.50	6.00	51	0.021	0.63	B
20C1	Proposed	C2	20	1	20.624	7.9890	6.0224	51.2901	0.0207	0.7661	B
	DIALux	C2	21.58	1	20.00	7.50	6.00	51	0.020	0.71	B
20C2	Proposed	C2	20	2	32.318	7.1288	8.9801	50.8340	0.0175	0.7018	B
	DIALux	C2	24.20	2	32.00	7.00	9.00	51	0.015	0.58	B
1.0M2	Proposed	M3	1.0	2	31.634	6.6372	9.8697	40.4714	0.0240	0.7035	B
	DIALux	M3	1.05	2	30.00	6.50	9.00	40	0.018	0.67	B
10C1	Proposed	C4	10	1	45.447	8.0344	6.1122	50.9523	0.0183	0.4157	B
	DIALux	C4	10.14	1	44.00	7.50	6.00	50	0.019	0.41	B
10C2	Proposed	C4	10	2	49.528	7.3539	9.9802	51.0252	0.0206	0.7813	B
	DIALux	C4	15.32	2	50.00	7.00	9.00	51	0.015	0.51	B
7.5P1	Proposed	P3	7.5	1	45.413	9.0992	6.9790	50.8924	0.0214	0.2527	B
	DIALux	P3	8.95	1	45.00	8.00	6.50	51	0.019	NA	B
7.5P2	Proposed	P3	7.5	2	48.288	7.5783	9.5217	41.2667	0.0239	0.3186	B
	DIALux	P3	8.31	2	48.00	8.00	9.50	40	0.019	NA	B

Table 12 Comparison between proposed model with existing approaches based on energy efficiency

Lighting class	Installation design factor (k)	Methodology	D_p	U_0	Energy class
C5	1	Existing [15]	0.023	0.40	B
		Proposed	0.018	0.43	B
C4	1	Existing [6]	0.027	0.20	C
		Proposed	0.017	0.40	B
C3	1	Existing [15]	0.023	0.66	B
		Proposed	0.018	0.42	B
	2	Existing [15]	0.014	0.06	A
		Proposed	0.014	0.41	A
C2	1	Existing [6]	0.026	0.71	C
		Proposed	0.019	0.70	B
C1	1	Existing [6]	0.023	0.75	B
		Proposed	0.015	0.65	B
	2	Existing [15]	0.015	0.61	B
		Proposed	0.013	0.45	A
P3	2	Existing [16]	0.028	-	C
		Proposed	0.019	-	B
P2	1	Existing [16]	0.033	-	C
		Proposed	0.021	-	B
P1	1	Existing [16]	0.040	-	D
		Proposed	0.018	-	B

To evaluate the performance of the proposed methodology, the results are also compared in accordance to the power of the luminaire. The outcome of the comparison depending on this power are summarized in Table 13. From this comparison, it is found that, the proposed methodology produces almost equal or somewhere more acceptable energy class by utilizing less power than the existing approaches [6, 15, 16]. This energy class indicates the energy efficiency of the lighting system as discussed earlier. Therefore, it can be said that, the proposed algorithm requires less power requirement to provide better energy efficiency than the existing algorithms. As discussed earlier, some of the parameters from the existing approaches violate the standardization recommendation which are represented with red cross mark in Table 13.

- *Comparison on energy consumption:*

The results obtained from the proposed algorithms are also compared over existing work on the basis of energy consumed by the lighting system. In this context, DIALux is used to acquire the values of energy consumption in a year by the specific instances. These values are then compared with an existing approach [14]. Here, the computations of the existing approach are performed on two road segments located in a residential area and middle of the city. Therefore, the energy consumption found on these two streets are compared with two instances namely 7.5P2 and 30C1 for pedestrian and conflict areas respectively. The energy consumption of the proposed approach obtained from DIALux is shown by Fig. 16. It is to be noted here that, the energy consumed by the existing approach [14] is based on different dimming lighting schemes which include conventional, part-night, dynadimmer

Table 13 Comparison between proposed model with existing approaches based on power requirement

Lighting class	Installation design factor (<i>k</i>)	Methodology	<i>P</i>	<i>S</i>	<i>H</i>	ω	D_p	U_0	Energy class
C5	1	Existing [15]	123	47	10	7	0.023	0.40	B
		Proposed	51	34	8	7	0.018	0.43	B
C4	1	Existing [6]	128	52.3	10	7	0.027	0.20	C
		Proposed	50	44	7.5	6	0.017	0.40	B
C3	1	Existing [15]	123	31	10	7	0.023	0.66	B
		Proposed	51	30	7	6	0.018	0.42	B
C3	2	Existing [15]	123	63	10	7	0.014	0.06	A
		Proposed	50	50	7	6.5	0.014	0.41	A
C2	1	Existing [6]	128	27.5	9.7	8	0.026	0.71	C
		Proposed	51	20	7.5	6	0.019	0.70	B
C1	1	Existing [6]	128	17.4	10	10	0.023	0.75	B
		Proposed	50	18	6	6	0.015	0.65	B
C1	2	Existing [15]	123	31.5	7	10	0.015	0.61	B
		Proposed	50	30	6	8	0.013	0.45	A
P3	2	Existing [16]	63	-	-	-	0.028	-	C
		Proposed	40	48	8	9.50	0.019	-	B
P2	1	Existing [16]	182	-	-	-	0.033	-	C
		Proposed	40	26	7	7	0.021	-	B
P1	1	Existing [16]	191	-	-	-	0.040	-	D
		Proposed	51	30	7	6	0.018	-	B

Name	Proposed(7.5P2)
Optimization	Results: 1
Light loss factor	0.670
Luminaire arrangement 1	DYANA LED 36L35 NR 730 CLO CL2 MA7I
Fitting	1 x LED 40 W
Pole distance [m]	48.000
Light centre height [m]	8.000
Boom angle [°]	0.0
Light overhang [m]	0.500
Pole rotation [°]	0.0
No. of luminaires per pole	1
Pole distance from roadway [m]	0.500
Boom length [m]	1.000
Wattage / km [W/km]	1680
Energy consumption [kWh/yr]	320
De [kWh/m ² /yr]	0.702
Dp [Dp (W/(lx*m ²))]	0.019
Valuation field (P3)	Roadway 1 (P3)
Em [lx]	✓ ≥ 7.50 ≤ 11.25 9.34 ✓
Emin [lx]	✓ ≥ 1.50 5.97 ✓

(a) 7.5P2

Name	Proposed (30C1)
Optimization	Results: 1
Light loss factor	0.670
Luminaire arrangement 1	R2L2 S 48L35 WS 740 CL1 [STD] (96268)
Fitting	1 x LED 50 W
Pole distance [m]	18.000
Light centre height [m]	6.000
Boom angle [°]	0.0
Light overhang [m]	0.500
Pole rotation [°]	0.0
No. of luminaires per pole	1
Pole distance from roadway [m]	0.500
Boom length [m]	0.560
Wattage / km [W/km]	2800
Energy consumption [kWh/yr]	200
De [kWh/m ² /yr]	1.85
Dp [Dp (W/(lx*m ²))]	0.015
Valuation field (C1)	Proposed (C1)
Em [lx]	✓ ≥ 30.00 30.37 ✓
Uo	✓ ≥ 0.40 0.75 ✓

(b) 30C1

Fig. 16 Energy consumption of two instances from DIALux

Table 14 Comparison between proposed model with existing approaches based on energy consumption

Instance	Methodology	Conventional Wh/day	Chronosense Wh/day	Part night Wh/day	Dynadimmer Wh/day
7.5P2	Existing [14]	1332.4	1166.2	809.2	809.2
	Proposed		320 kWh/yr = 320,000/365 = 876.7123 Wh/day		
30C1	Existing [14]	1254.4	1097.6	761.6	761.6
	Proposed		200 kWh/yr = 200,000/365 = 547.9452 Wh/day		

etc., as well as a sensor-based approach. However, all the computations considered in the proposed approach is performed by assuming a conventional lighting system. Hence, to perform a fair comparison, the sensor-based approach in the existing methodology is ignored and the computed energy consumption for the rest of the lighting schemes are compared with the results of the MOEA in the proposed methodology as shown in Table 14. In this table, it can be found that, the energy consumption obtained from the instance 7.5P2 is less than conventional and chronosense lighting schemes whereas it consumes a little higher energy than part night and dynadimmer schemes. It is due to the arrangement of lighting in part night and dynadimmer. Here, the proposed methodology maintains a two-sided uniform lighting arrangement whereas in case of existing approach the installation of two-sided lighting configuration is not arranged uniformly. Again, the input power supply of the streetlights for the existing approach is found to be insufficient to maintain a minimum threshold of the power requirement. However, the energy consumption obtained from the instance 30C1 is less than all of the lighting schemes presented here. Therefore, the proposed conventional street lighting system consumes less energy than some of the existing dimming lighting schemes for one-sided installation configuration.

8 Conclusion

In this paper, an energy efficient street lighting framework is designed to maximize the energy efficiency and uniformity of the lighting system. The framework provides the lighting design guidelines for obtaining an energy efficient system while satisfying the CIE recommendation. Here, different MOEAs such as NSGAIL, SPEA2 and MODEA are used on each of the lighting instances that include different lighting class. The results of these MOEAs are analysed based on the performance metrics like GD, IGD, space, spread, HV and MPFE. From the analysis, it is concluded that NSGAIL performs better than SPEA2 and MODEA in

preserving the diversity of the solutions where the convergence is maintained overall same in all of the MOEAs used in this proposed framework. This data analysis is particularly useful to easily determine a suitable solution in terms of energy efficiency, which can provide a quick method to design sustainable installations of the street lights. The performance of NSGAIL is compared with DIALux to validate the results obtained by the framework proposed here. Thus, this result validation has contributed a significant role in designing energy efficient street lighting. Therefore, the novelty and originality of this energy efficient street lighting framework are derived from the results obtained of our current study as:

- The energy efficiency obtained by the proposed work is expressed by the performance of several MOEAs in terms of fundamental properties of Pareto fronts which is not yet discussed in any MOO based existing approach related to street lighting installation. Furthermore, existing works in this domain often introduces only few metrics to estimate the performance based on the results from benchmarks which show incompleteness in evaluation. Henceforth, the performance of the proposed work is assessed with respect to a complete set of metrics for a possible combination of various parameters related to different lighting classes. Here, the proposed data analysis approach in this paper is found to be more converged and with better diversity in terms of performance measures like GD, IGD, space, spread, HV and MPFE.
- For verifying the applicability of the proposed work, it is presented based on several instances that include the lighting classes and the installation configuration as per characteristics of specific streets under a single platform, which is beyond the scope of the existing works.
- The energy efficiency of the system is determined by the energy class which is a series of "A" to "G", in which the energy class "A" is most energy efficient while "G" represents the least. From thorough literature survey, it is found that, the energy classes of the existing works are in the range of B to G whereas, the proposed

MOEAs approached in this paper have significantly attain an improved energy class from the range A to C.

- After the post processing of data obtained in simulations, a comprehensive data analysis is contributed. It provides a detailed statistical analysis on the performance metrics in various aspects as well the Pare-to front search results with useful insights. Consequently, the convincing results obtained by data analysis can assist the stakeholders in designing an energy efficient street lighting. Hence, it is important to mention here that no prior work based on the utilization of data analysis is there in the literature for designing a street lighting framework.

From a theoretical point of view, it contributes to the literature on multi-objective studies through a comprehensive data analysis approach for obtaining an energy efficient solution in street lighting management. Hence, by considering its exclusiveness, the proposed methodology may be applied to different street lighting contexts, namely to contexts characterized by diverse objectives, constraints, and performance as well as implementation criteria in practice. However, to include new and competing objectives, which can descend from new strategies formulated by the energy managers, future research may focus on the development of the Internet of Things (IoT) based energy efficient street lighting framework.

Declarations

Ethical Approval This article does not contain any studies with human participants or animals performed by any of the authors.

Informed Consent Informed consent was obtained from all participants included in the study.

Conflict of interest All authors of this research paper declare that they have no conflict of interest.

References

1. Kyba CCM, Hänel A, Hölker F (2014) Redefining efficiency for outdoor lighting. *Energy Environ Sci* 7(6):1806–1809. <https://doi.org/10.1039/C4EE00566J>
2. Atkins S, Husain S, Storey A (1991) The influence of street lighting on crime and fear of crime. Crime Prevention Unit
3. Lau SP, Merrett GV, White NM (2013) Energy-efficient street lighting through embedded adaptive intelligence. In: 2013 International Conference on Advanced Logistics and Transport. IEEE, pp 53–58
4. Sikdar PL, Thakurta PKG (2021) An energy efficient street lighting framework: Ann-based approach. *Innov Syst Softw Eng* 17:131–139. <https://doi.org/10.1007/s11334-020-00375-2>
5. Alzubaidi S, Soori PK (2012) Study on energy efficient street lighting system design. In: 2012 IEEE International Power Engineering and Optimization Conference Melaka, Malaysia. IEEE, pp 291–295
6. Rabaza O, Gómez-Lorente D, Pozo AM, Pérez-Ocón F (2019) Application of a differential evolution algorithm in the design of public lighting installations maximizing energy efficiency. *LEUKOS*. <https://doi.org/10.1080/15502724.2019.1568255>
7. on Illumination IC (2010) Lighting of roads for motor and pedestrian traffic. CIE Public 115. <https://cie.co.at/publications/lighting-roads-motor-and-pedestrian-traffic>
8. for Standardization EC (2015) Road lighting - part 5: Energy performance indicators. In European Committee for Standardization, CEN EN 13201: 5. <https://standards.iteh.ai/catalog/standards/cen/704740a6-0a29-432c-a6f1-0ed85400f9d3/en-13201-5-2015>
9. GmbH D Dialux - dial. <https://www.dial.de/en/dialuxx>
10. Doulos LT, Sioutis I, Kontaxis P, Zissis G, Faidas K (2019) A decision support system for assessment of street lighting tenders based on energy performance indicators and environmental criteria: Overview, methodology and case study. *Sustain Cit Soc* 51:101759. <https://doi.org/10.1016/j.scs.2019.101759>
11. Gómez-Lorente D, Rabaza O, Estrella AE, Peña-García A (2013) A new methodology for calculating roadway lighting design based on a multi-objective evolutionary algorithm. *Expert Syst Appl* 40(6):2156–2164. <https://doi.org/10.1016/j.eswa.2012.10.026>
12. Coello CAC, Lamont GB, Van Veldhuizen DA et al (2007) Evolutionary algorithms for solving multi-objective problems. vol 5. Springer. <https://www.cs.cinvestav.mx/~emoobook/>
13. Yu X, Lu Y, Yu X (2018) Evaluating multiobjective evolutionary algorithms using mcdm methods. *Math Probl Eng*. <https://doi.org/10.1155/2018/9751783>
14. Dizon E, Pranggono B (2021) Smart streetlights in smart city: a case study of sheffield. *J Ambient Intell Human Comput*:1–16
15. Rabaza O, Gómez-Lorente D, Pérez-Ocón F, Peña-García A (2016) A simple and accurate model for the design of public lighting with energy efficiency functions based on regression analysis. *Energy* 107:831–842. <https://doi.org/10.1016/j.energy.2016.04.078>
16. Rabaza O, Molero-Mesa E, Aznar-Dols F, Gómez-Lorente D (2018) Experimental study of the levels of street lighting using aerial imagery and energy efficiency calculation. *Sustainability* 10(12):4365
17. Sikdar PL, Thakurta PKG (2020) An improved energy-efficient street lighting system. In: 2020 7th International Conference on Signal Processing and Integrated Networks (SPIN). IEEE, pp 372–376
18. Lau SP, Merrett GV, Weddell AS, White NM (2015) A traffic-aware street lighting scheme for smart cities using autonomous networked sensors. *Comput Electr Eng* 45:192–207. <https://doi.org/10.1016/j.compeleceng.2015.06.011>
19. Sikdar PL, Thakurta PKG (2020) An energy efficient autonomous street lighting system, pp 589–599. https://doi.org/10.1007/978-981-15-2188-1_46
20. Wicaksono HIS, Abdullah AG, Hakim DL (2021) Optimizing public street lighting and redesign of public road lighting based on dialux and fuzzy logic. In: IOP Conference Series: Materials Science and Engineering, vol 1098. IOP Publishing, p 042013
21. Campisi D, Gitto S, Morea D et al (2017) Light emitting diodes technology in public light system of the municipality of rome: An economic and financial analysis. *Int J Energy Econ Policy* 7(1):200–208
22. Abdullah AG, Aziz M, Huda MN (2021) Redesigning public street lighting using photometric method. *Ind J Comput Eng Des (IJoCED)* 3(1):54–67. <https://doi.org/10.35806/ijoced.v3i1.153>
23. Räsänen T, Ruuskanen J, Kolehmainen M (2008) Reducing energy consumption by using self-organizing maps to create more

- personalized electricity use information. *Appl Energy* 85(9):830–840. <https://doi.org/10.1016/j.apenergy.2007.10.012>
24. Sánchez-Balvás LA, de Felipe JJ, Quintero JM, de la Fuente A (2021) An energy efficiency-based classification approach for street lighting by considering operational factors: a case study of barcelona. *Energy Efficiency* 14(1):1–32. <https://doi.org/10.1007/s12053-020-09915-y>
 25. Garcés-Jimenez A, Castillo-Sequera JL, Del Corte-Valiente A, Gómez-Pulido JM, González-Seco EPD (2019) Analysis of artificial neural network architectures for modeling smart lighting systems for energy savings. *IEEE Access* 7:119881–119891. <https://doi.org/10.1109/ACCESS.2019.2932055>
 26. Guo Z, Shen Y, Bashir AK, Yu K, Lin JC (2021) Graph embedding-based intelligent industrial decision for complex sewage treatment processes. *Int J Intell Syst*
 27. Ożadowicz A, Grela J (2017) Energy saving in the street lighting control system—a new approach based on the en-15232 standard. *Energy Efficiency* 10(3):563–576. <https://doi.org/10.1007/s12053-016-9476-1>
 28. Lin JC-W, Srivastava G, Zhang Y, Djenouri Y, Aloqaily M (2020) Privacy-preserving multiobjective sanitization model in 6g iot environments. *IEEE Internet Things J*. 8(7):5340–5349
 29. Yong Z, Li-Juan Y, Qian Z, Xiao-Yan S (2020) Multi-objective optimization of building energy performance using a particle swarm optimizer with less control parameters. *J Build Eng* 32:101505
 30. Wang C-S, Li B-Y, Yang C-W, Lin W-C, Hung S-C, Chiang S-B, Tsuei C-H (2019) Optimized luminaire allocation and configuration with luminaire failure compensation. In: 2019 IEEE International Conference on Big Data and Smart Computing (BigComp). IEEE, pp 1–8
 31. Rabaza O, Peña-García A, Pérez-Ocón F, Gómez-Lorente D (2013) A simple method for designing efficient public lighting, based on new parameter relationships. *Expert Syst Appl* 40(18):7305–7315. <https://doi.org/10.1016/j.eswa.2013.07.037>
 32. Gómez-Lorente D, Rabaza O, Espín A, Peña-García A (2013) Optimization of efficiency and energy saving in public lighting with multi-objective evolutionary algorithms. In: *Proceedings of ICREPQ*, pp 1–4
 33. Shao Y, Lin JC-W, Srivastava G, Guo D, Zhang H, Yi H, Jolfaei A (2021) Multi-objective neural evolutionary algorithm for combinatorial optimization problems. *IEEE Transactions on Neural Networks and Learning Systems*
 34. Meng D, Xiao Y, Guo Z, Jolfaei A, Qin L, Lu X, Xiang Q (2021) A data-driven intelligent planning model for uavs routing networks in mobile internet of things. *Comput Commun* 179:231–241
 35. Liu H, Li Y, Duan Z, Chen C (2020) A review on multi-objective optimization framework in wind energy forecasting techniques and applications. *Energy Convers Manag* 224:113324
 36. Rabaza O, Palomares-Muñoz ZE, Peña-García A, Gómez-Lorente D, Arán-Carrión J, Aznar-Dols F, Espín-Estrella A (2014) Multi-objective optimization applied to photovoltaic street lighting systems. *Proc. IEEE ICREPQ*, ISSN, pp 2172–038. <https://doi.org/10.24084/repqj12.419>
 37. Jalali Z, Noorzai E, Heidari S (2020) Design and optimization of form and façade of an office building using the genetic algorithm. *Sci Technol Built Environ* 26(2):128–140. <https://doi.org/10.1080/23744731.2019.1624095>
 38. Nath AS, Pal A, Mukhopadhyay S, Mondal KC (2019) A survey on cancer prediction and detection with data analysis. *Innov Syst Softw Eng*:1–13. <https://doi.org/10.1007/s11334-019-00350-6>
 39. St L, Wold S et al (1989) Analysis of variance (anova). *Chemometrics Intell Lab Syst* 6(4):259–272. [https://doi.org/10.1016/0169-7439\(89\)80095-4](https://doi.org/10.1016/0169-7439(89)80095-4)
 40. Lindsey JL (1997) *Applied illumination engineering*. The Fairmont Press, Inc.
 41. Deb K, Pratap A, Agarwal S, Meyarivan TAMT (2002) A fast and elitist multiobjective genetic algorithm: Nsga-ii. *IEEE Trans Evol Comput* 6(2):182–197. <https://doi.org/10.1109/4235.996017>
 42. Gharari R, Poursalehi N, Abbasi M, Aghaie M (2016) Implementation of strength pareto evolutionary algorithm ii in the multiobjective burnable poison placement optimization of kwu pressurized water reactor. *Nucl Eng Technol* 48(5):1126–1139. <https://doi.org/10.1016/j.net.2016.04.004>
 43. King RTFAh, Deb K, Rughooputh HCS (2010) Comparison of nsga-ii and spea2 on the multiobjective environmental/economic dispatch problem. *Univ Mauritius Res J* 16(1):485–511. <https://www.ajol.info/index.php/umrj/article/view/131124>
 44. Zitzler E, Laumanns M, Thiele L (2001) *Spea2: Improving the strength pareto evolutionary algorithm*. TIK-report 103. <https://doi.org/10.3929/ethz-a-004284029>
 45. Sreedhar D, Rajan BMR (2013) Differential evolution based multi-objective optimization—a review. *Int J Comput Appl* 63(15):14–19
 46. Gujarathi AM, Babu BV et al (2009) Improved strategies of multi-objective differential evolution (mode) for multi-objective optimization. In: *IICAI*, pp 933–948
 47. Barma PS, Dutta J, Mukherjee A, Kar S (2021) A multi-objective ring star vehicle routing problem for perishable items. *J Ambient Intell Human Comput*:1–26. <https://doi.org/10.1007/s12652-021-03059-2>
 48. Van Veldhuizen DA, Lamont GB (1998) *Multiobjective evolutionary algorithm research: A history and analysis*. Technical Report, Citeseer
 49. Schott JR (1995) *Fault tolerant design using single and multicriteria genetic algorithm optimization*. Ph.D. Thesis, Massachusetts Institute of Technology
 50. Zitzler E, Thiele L (1998) *Multiobjective optimization using evolutionary algorithms—a comparative case study*. In: *International conference on parallel problem solving from nature*. Springer, pp 292–301
 51. Jiang C, Zhang Z, Han X, Liu J (2013) A novel evidence-theory-based reliability analysis method for structures with epistemic uncertainty. *Comput Struct* 129:1–12. <https://doi.org/10.1016/j.compstruc.2013.08.007>
 52. Dutta J, Barma PS, Mukherjee A, Kar S, De T (2020) A multi-objective open set orienteering problem. *Neural Comput Appl* 32(17):13953–13969. <https://doi.org/10.1007/s00521-020-04798-7>

Publisher's note Springer Nature remains neutral with regard to jurisdictional claims in published maps and institutional affiliations.